



Cepheids and RR Lyrae in the Gaia-NIR perspective

M. Marconi & V. Ripepi

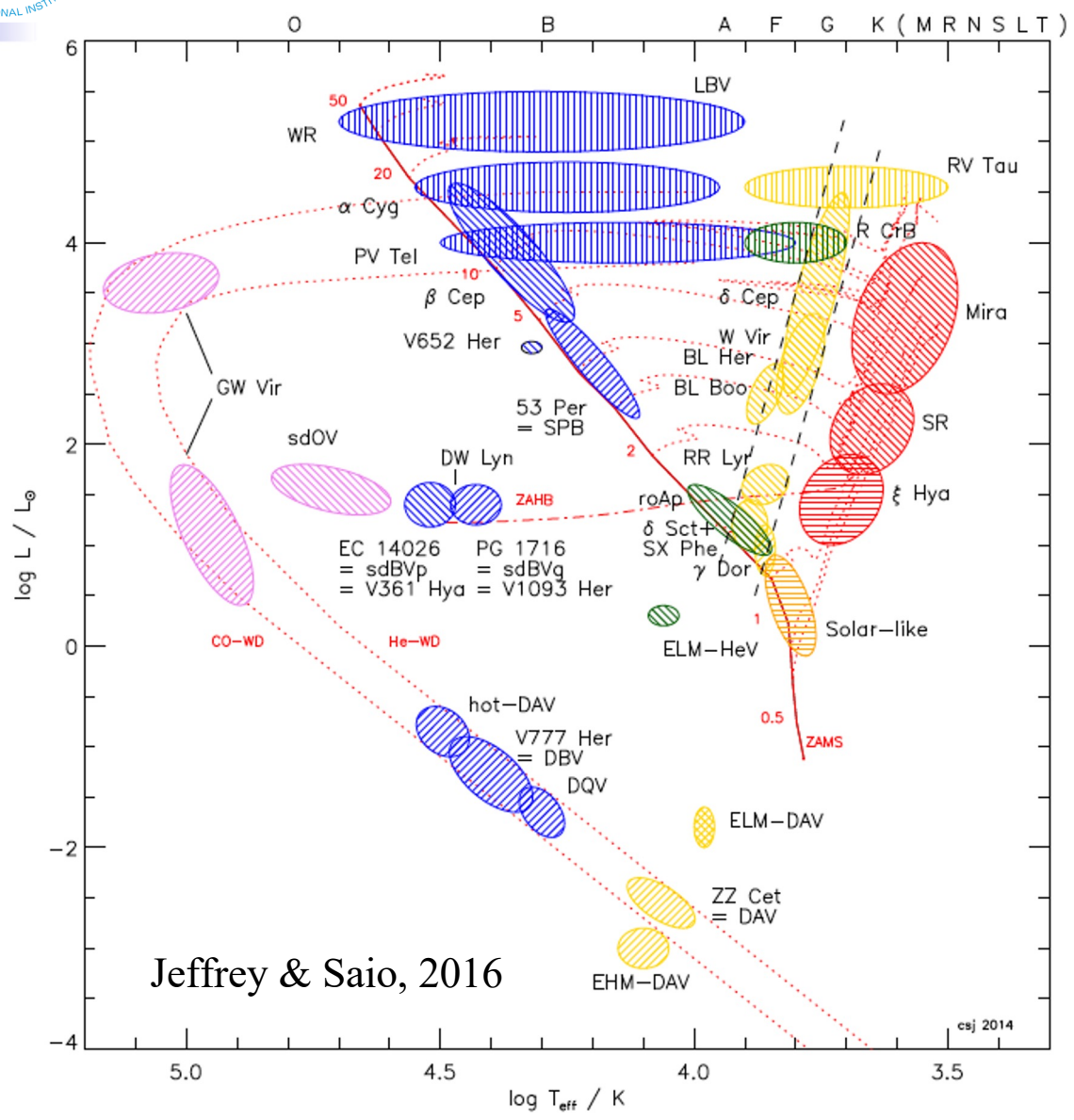
INAF-Osservatorio Astronomico di Capodimonte

Thanks to G. Clementini, S. Leccia, R. Molinaro, I. Musella, G. De Somma, L. Eyer and all the Gaia DPAC CU7 team

Outline

- The relevance of Cepheids and RR Lyrae
- Cepheids and RR Lyrae in the Gaia DR3 catalogue
- Model predictions for Cepheids and RR Lyrae
- The Gaia-NIR perspective

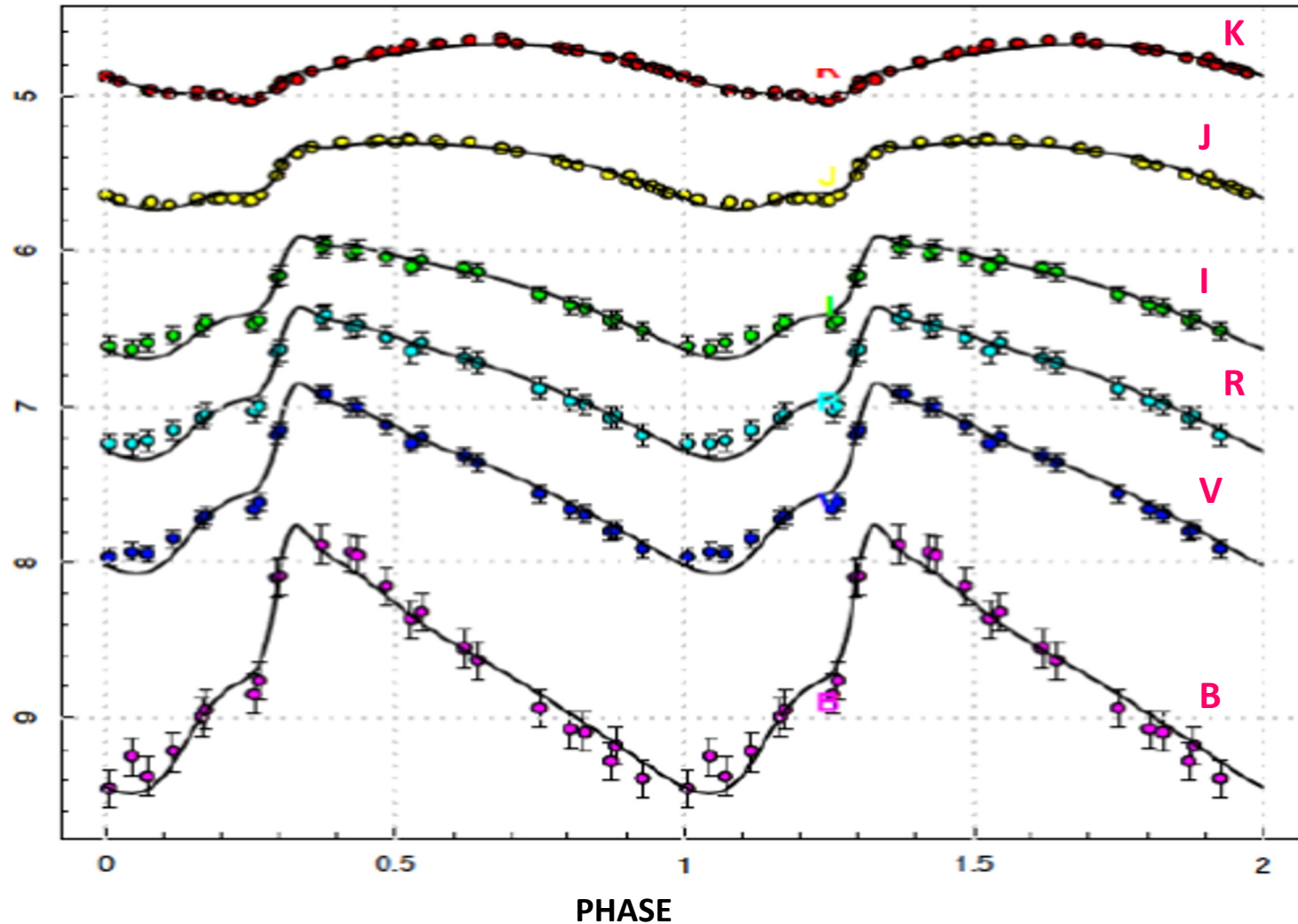
Cepheids and RR Lyrae are pulsating stars



They lie in the "classical" instability strip.

Their pulsation mechanism is associated to opacity variations within the H, He and He⁺ ionization regions.

Classical Cepheids



Classical Cepheids: central helium burning stars ($M=3\div 13M_{\odot}$, $M_V = -2\div -7$ mag, $P=1\div 100$ d; 50÷500 Myrs).

Pulsate in F, 1O, 2O, Multiple modes.

High amplitudes of variations in the optical (~ 1 mag) \rightarrow easy to identify even at long distances.

Classical Cepheids as distance indicators

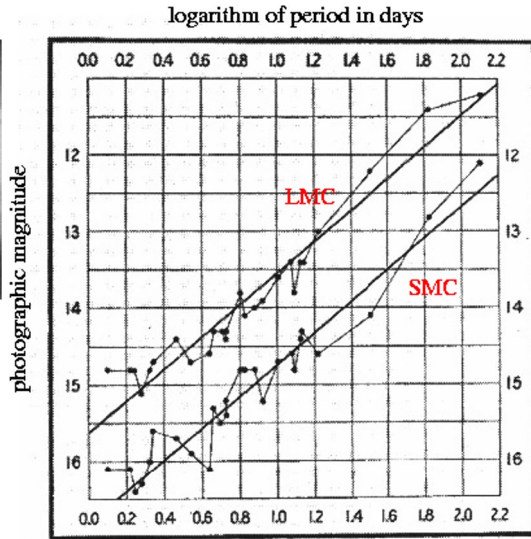
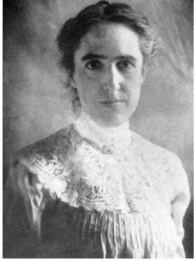
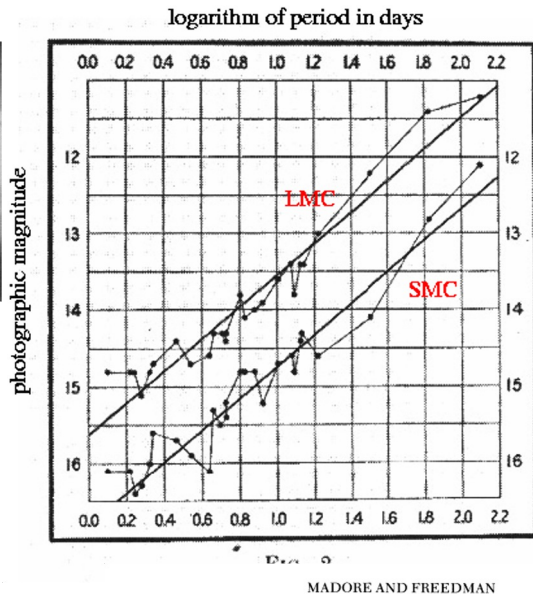


FIG. 2.

Since the discovery by Miss Leavitt (1908, 1912) in the SMC, Classical Cepheids are known to obey to a Period-Luminosity (P-L) relation.

→ Calibration of the extragalactic distance scale

Classical Cepheids as distance indicators

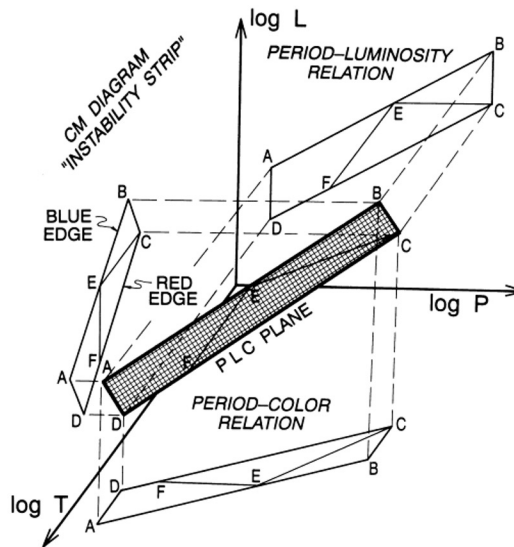


Since the discovery by Miss Leavitt (1908, 1912) in the SMC, Classical Cepheids are known to obey to a Period-Luminosity (P-L) relation.

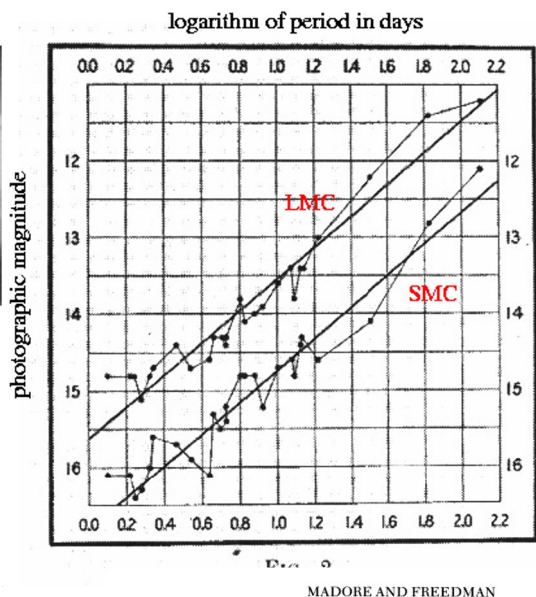
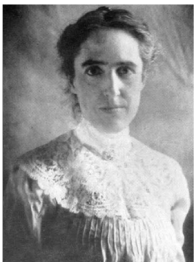
→ Calibration of the extragalactic distance scale

But the strip has a finite width → the PL relation is obtained from averaging over the color extension of the strip or, as early suggested by Madore & Freedman (1991) the PL is the projection of the PLC relation onto the PL plane.

The PL is a statistical relation !!



Classical Cepheids as distance indicators

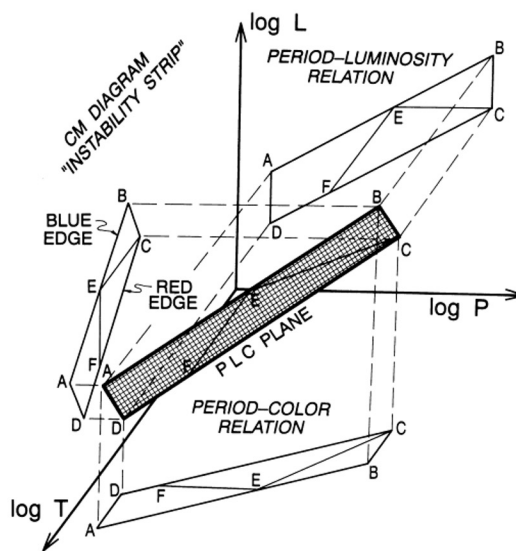


Since the discovery by Miss Leavitt (1908, 1912) in the SMC, Classical Cepheids are known to obey to a Period-Luminosity (P-L) relation.

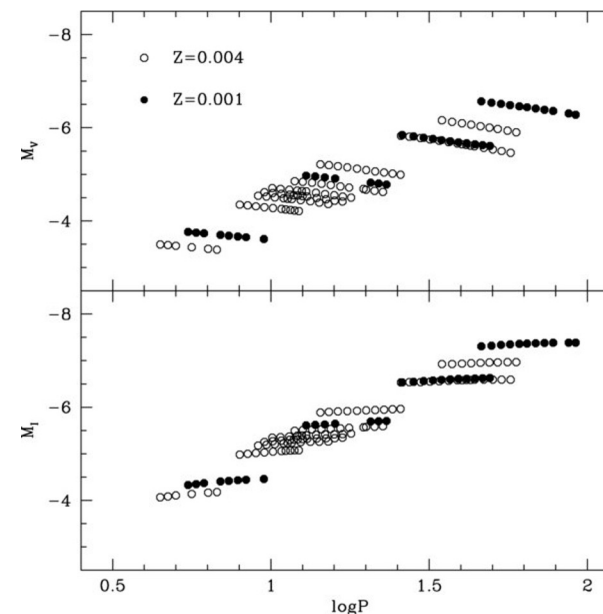
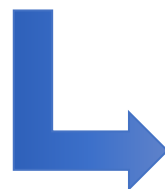
→ Calibration of the extragalactic distance scale

But the strip has a finite width → the PL relation is obtained from averaging over the color extension of the strip or, as early suggested by Madore & Freedman (1991) the PL is the projection of the PLC relation onto the PL plane.

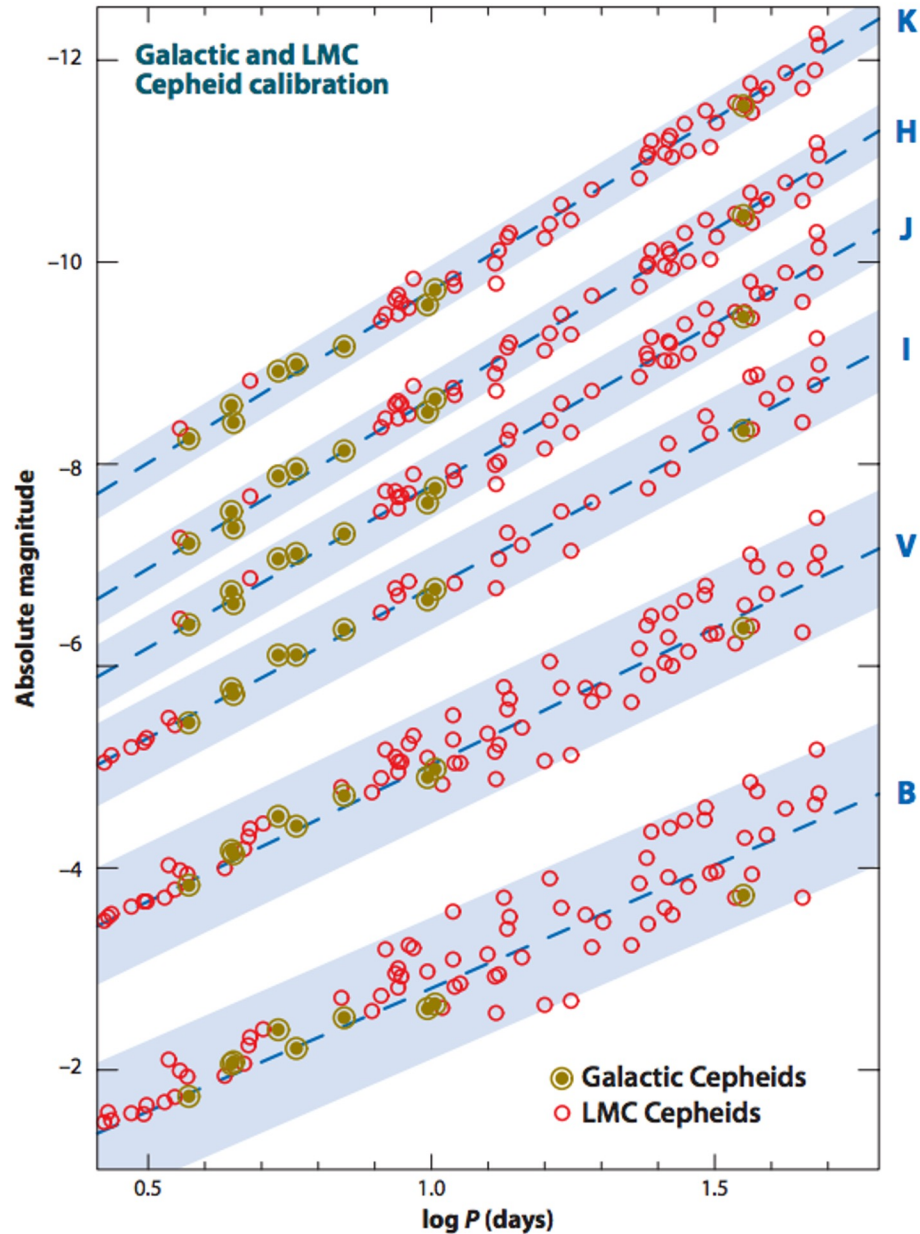
The PL is a statistical relation !!



Nonlinear convective pulsation models confirm that the topology of the instability strip reflects into the PL



Classical Cepheids as distance indicators



The intrinsic dispersion due to the finite width of the instability strip as well as to possible metallicity and reddening differences reduces when moving from the optical to the NIR filters.

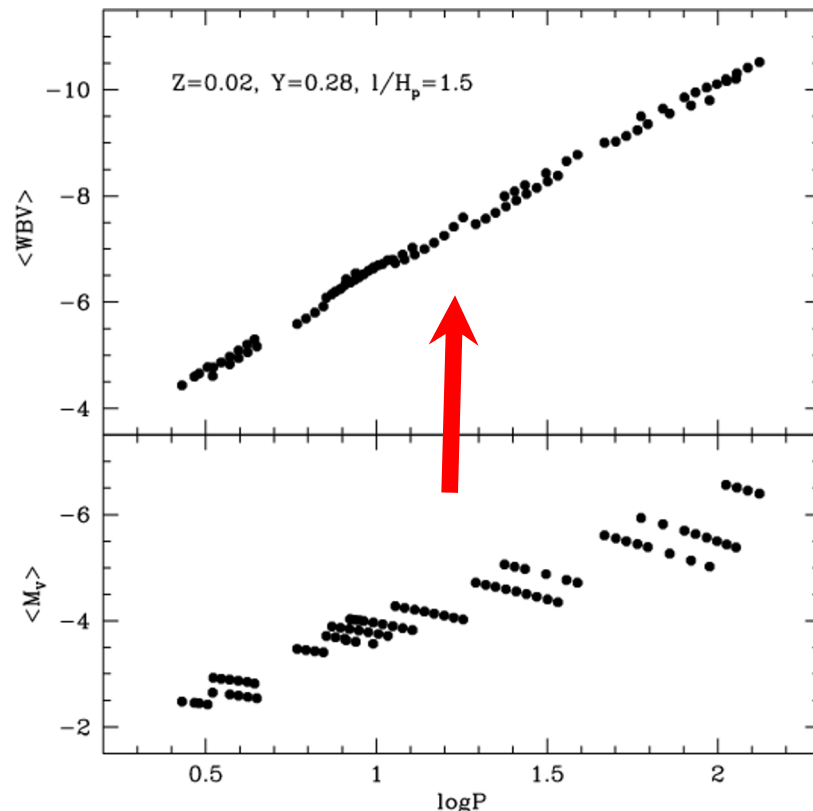
Freedman & Madore, 2010

Classical Cepheids as distance indicators

To avoid the effect of the finite width of the instability strip (especially in the optical bands) the Wesenheit function is often adopted:

$$\langle WBV \rangle = V - \gamma(B - V) \quad \gamma = A_V / E(B - V)$$

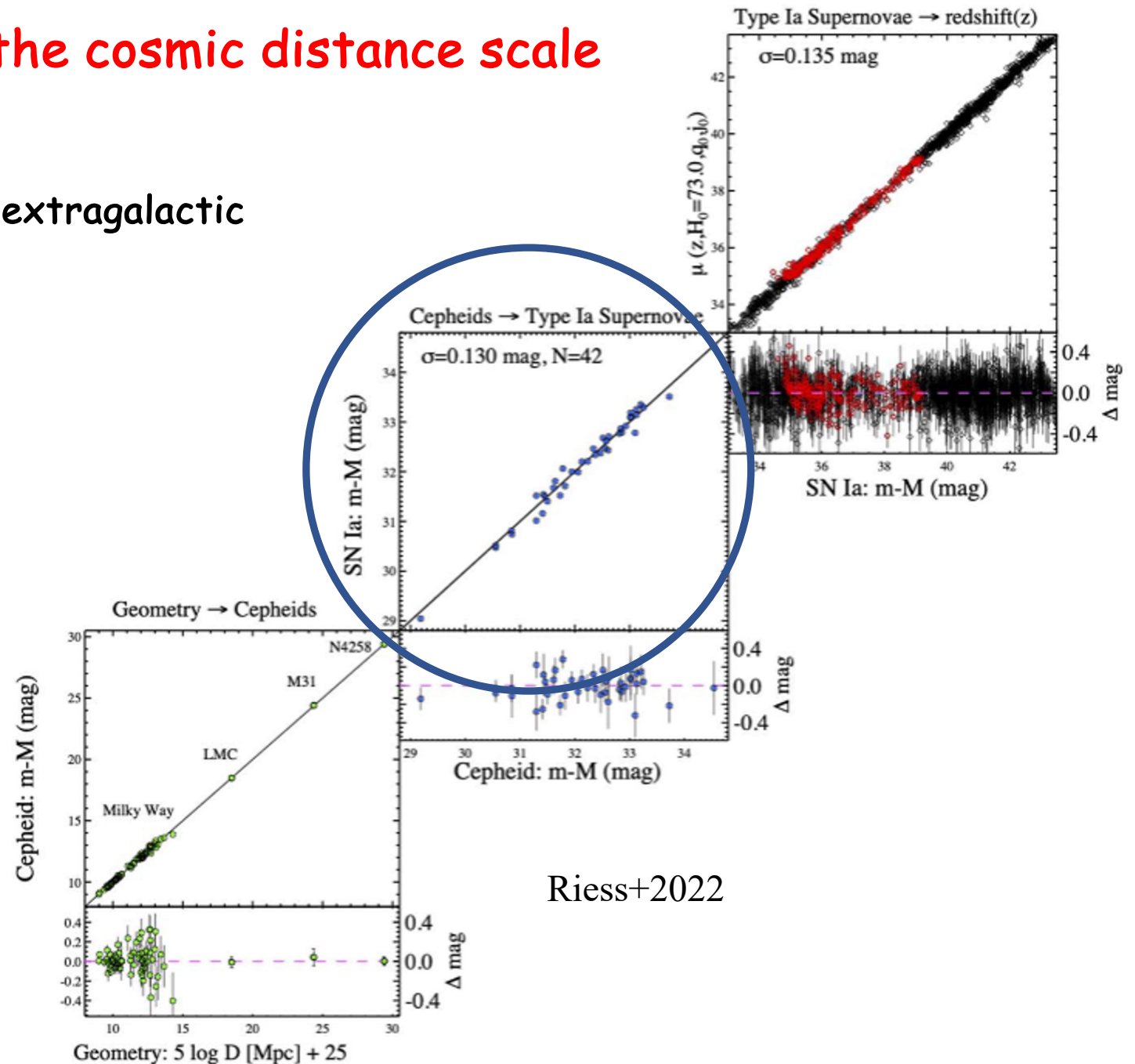
The **Period-Wesenheit (PW)** relation is not as rigorous as the PLC but is reddening free by definition.



Fiorentino, Marconi et al. 2007, A&A

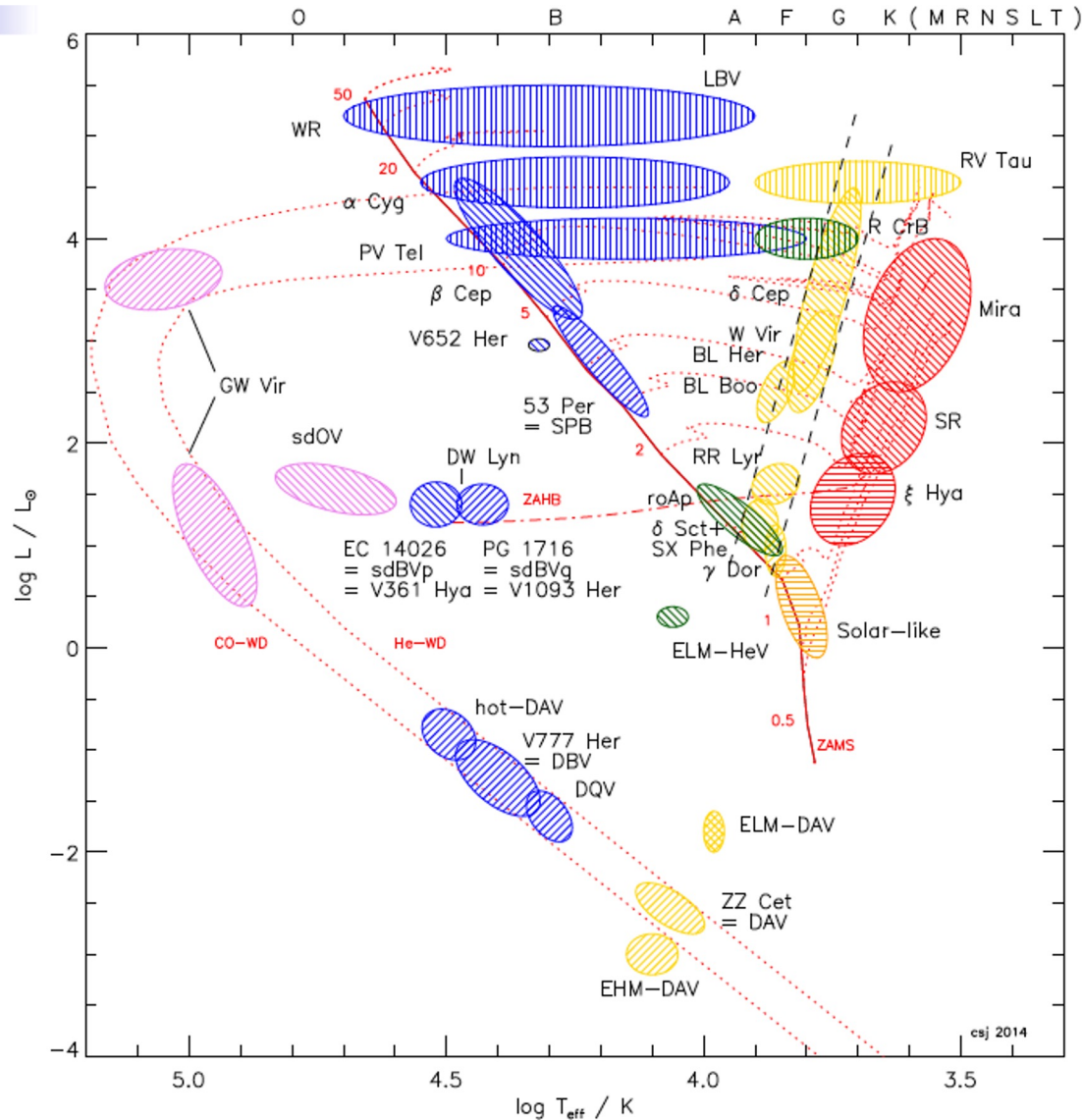
Cepheid stars as calibrators of the cosmic distance scale

- Most important standard candle in the extragalactic distance scale used to measure H_0 .



Riess+2022

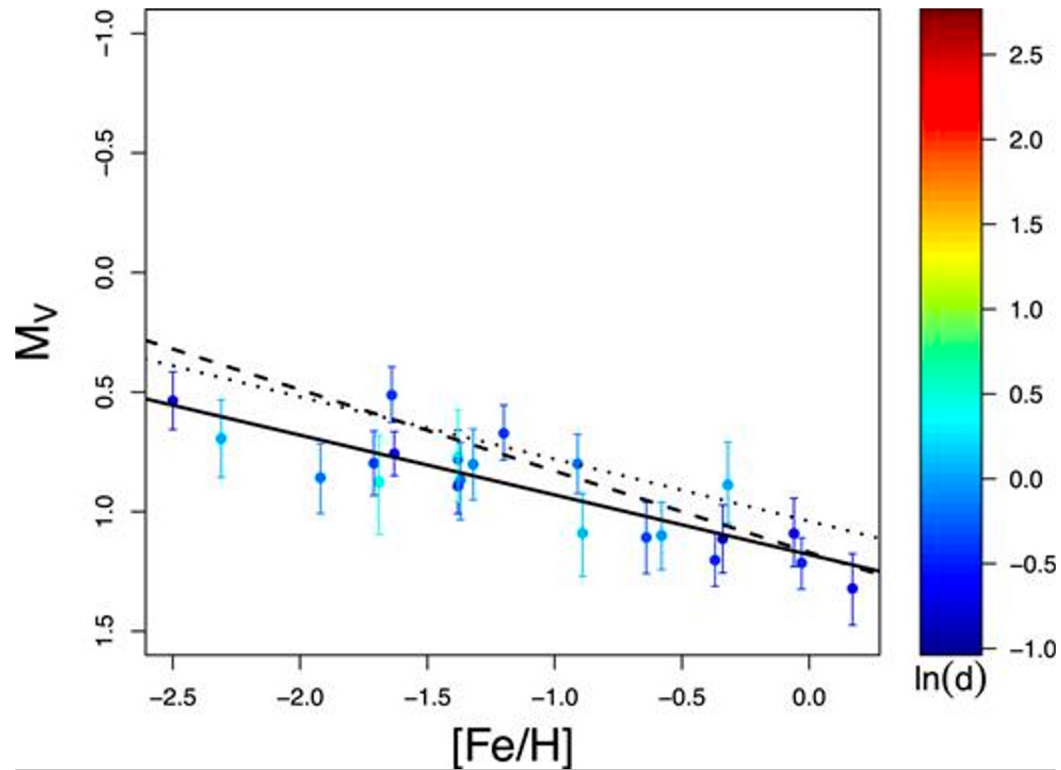
RR Lyrae stars



- Old ($t > 10$ Gyr) low mass ($0.52 < M_0 < 0.80$) central helium burning stars.
- Periods $0.2 < P$ (d) < 1.0
- $M_v \sim 0.6$ mag
- RRab, RRc, RRd (F, 10, mixed F/10 modes)
- Follow M_v -[Fe/H] relation in the optical and PLZ relations in the near-infrared

RR Lyrae stars as distance indicators

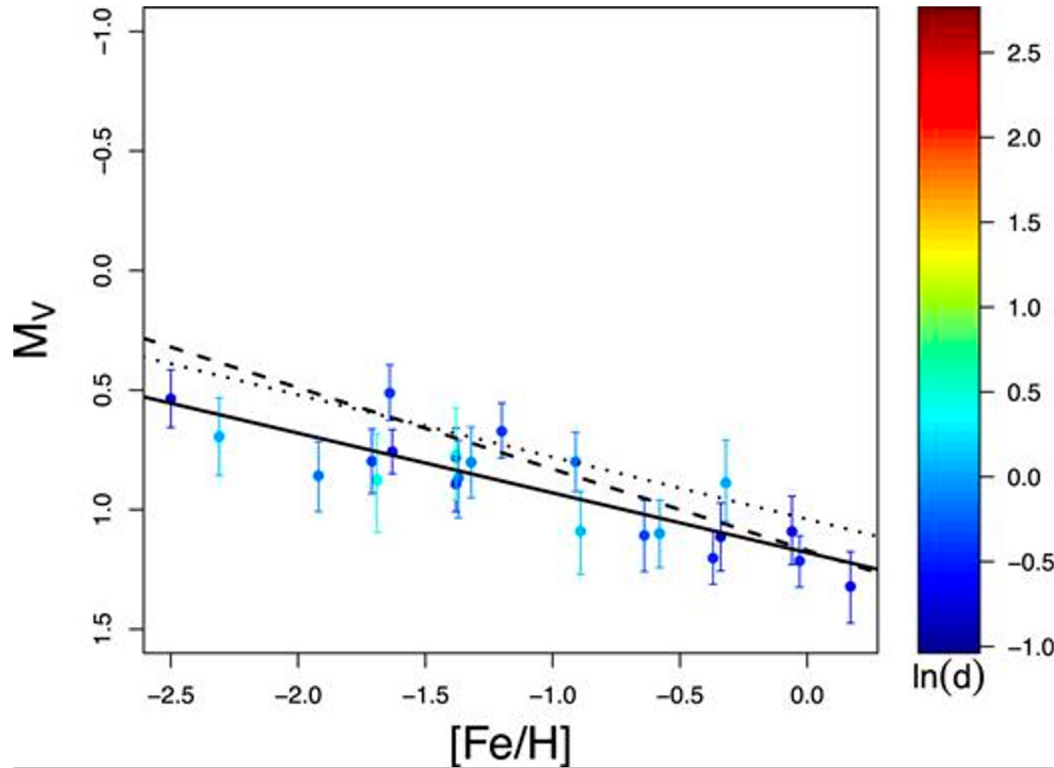
The M_V (RR)-[Fe/H] relation



Muraveva et al. 2018, MNRAS

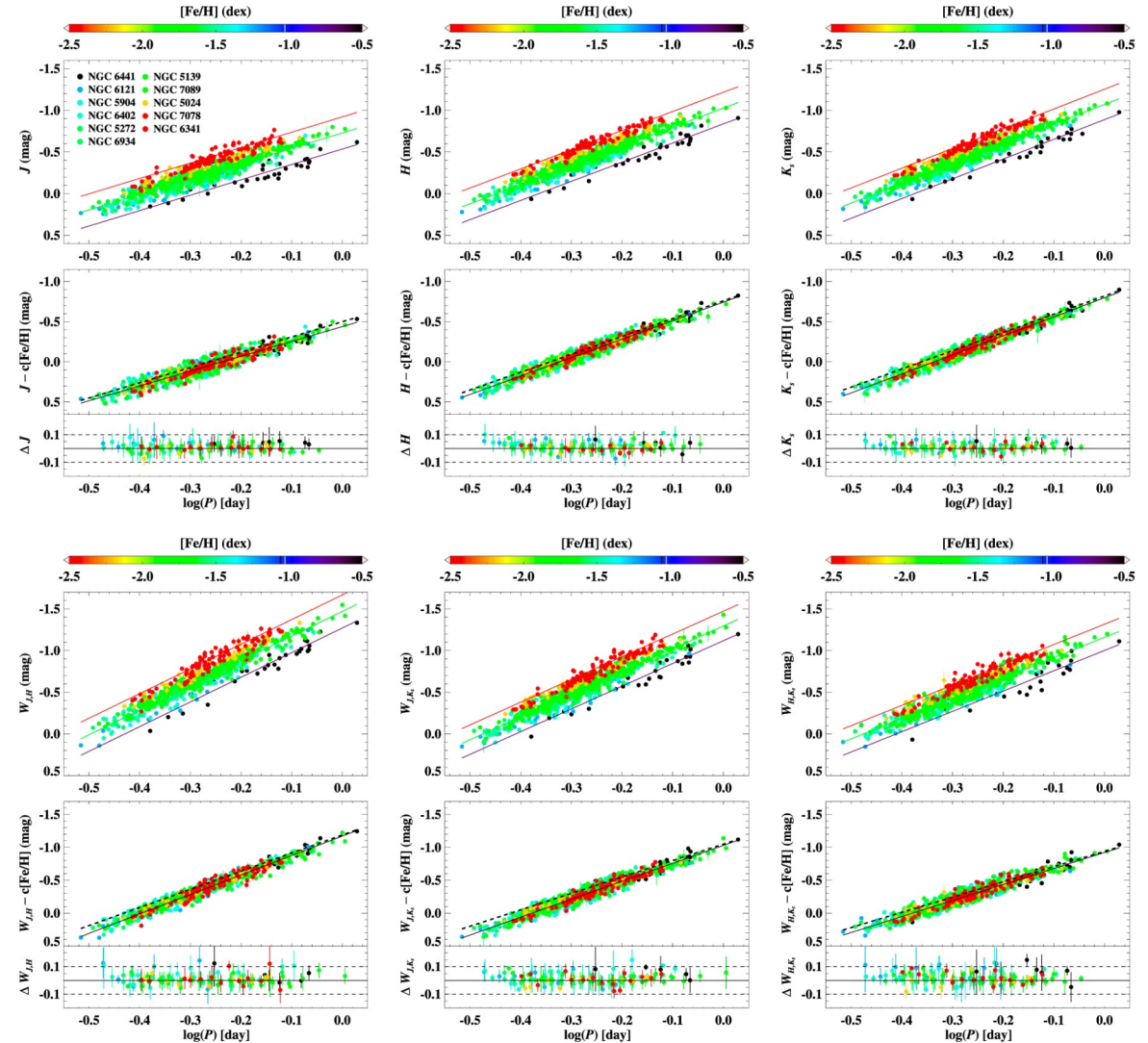
RR Lyrae stars as distance indicators

The $M_V(\text{RR})$ -[Fe/H] relation



Muraveva et al. 2018, MNRAS

The NIR P-L-[Fe/H] relations and the P-W-[Fe/H] relations

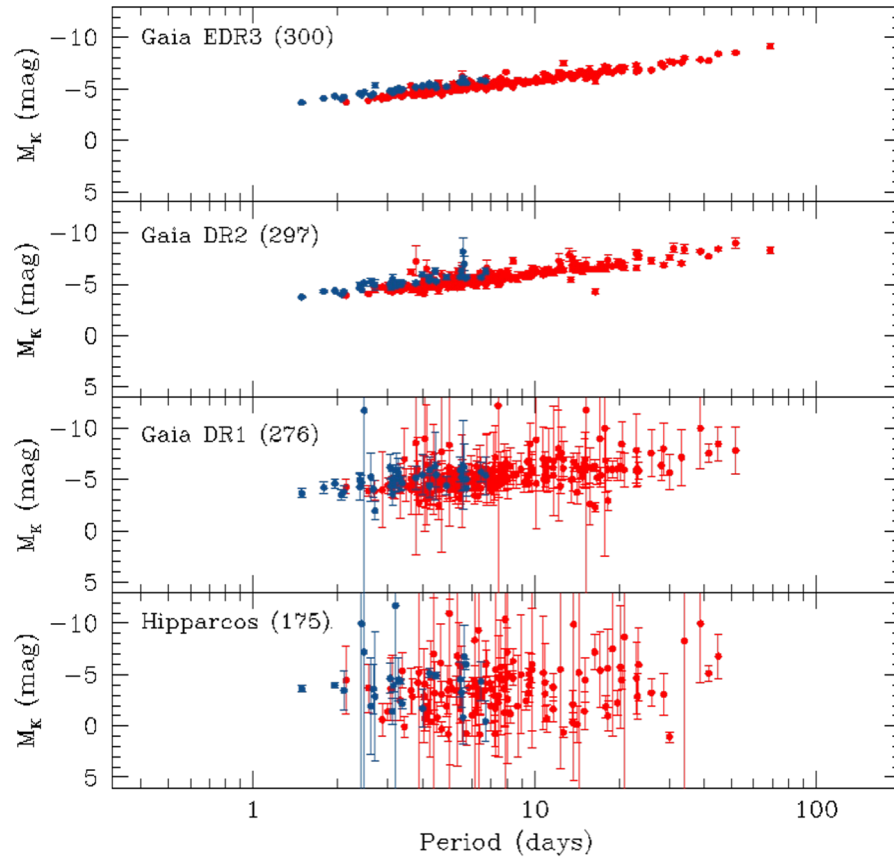


Bhardwaj et al. 2023, ApJL

Gaia: the game changer

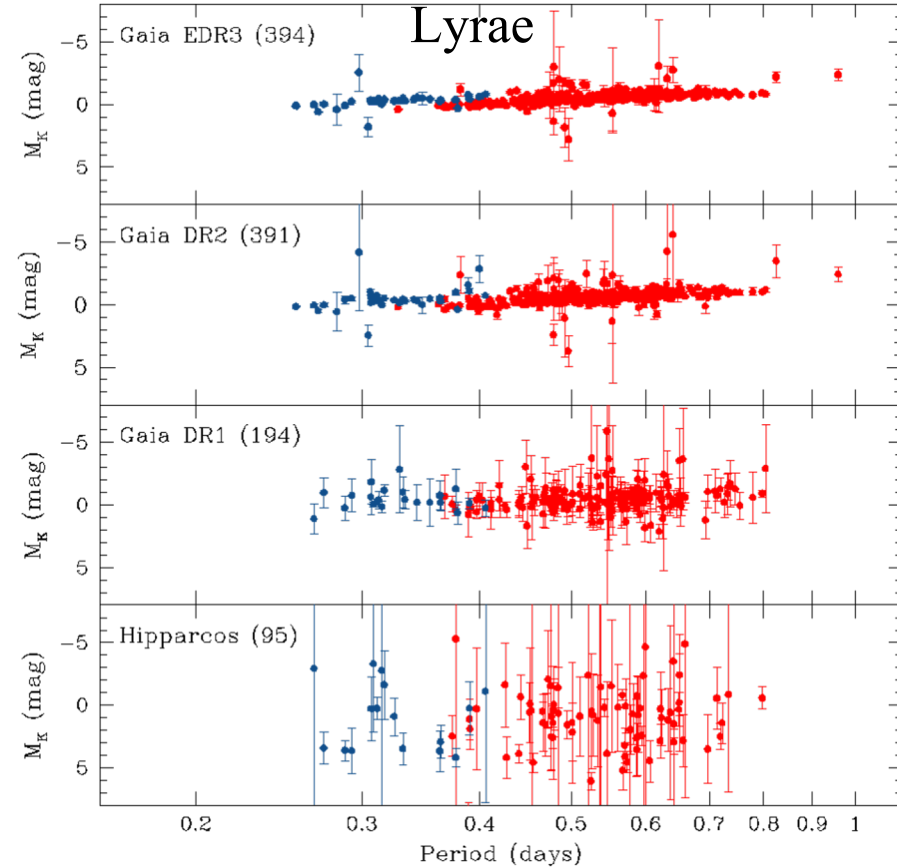
NIR PL relations of Cepheids and RR Lyrae before and after Gaia

Cepheids



Credit: ESA/Gaia/DPAC, created by: V. Ripepi

RR



Credit: ESA/Gaia/DPAC, created by: T. Muraveva & A. Garofalo

Variable sources in DR3 distributed in main types

- AGN
- Rotation (+other)
- Eruptive/Cataclysmic
- Pulsation
- Eclipsing systems
- Other

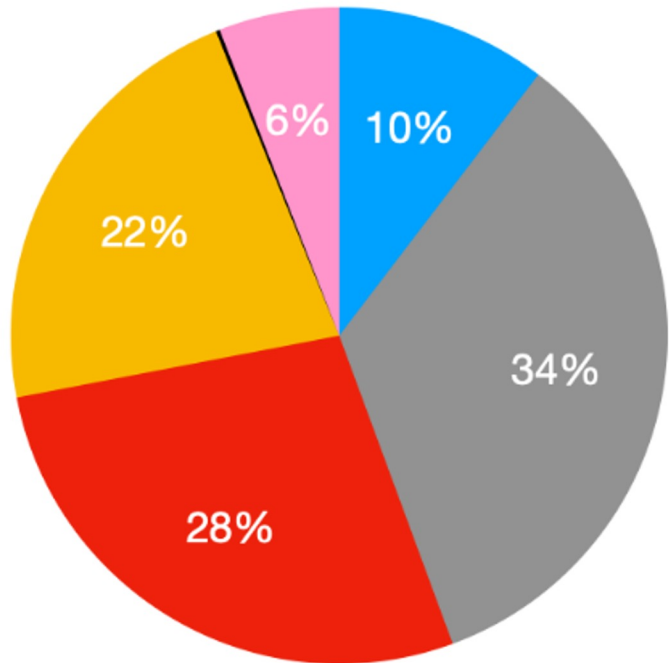
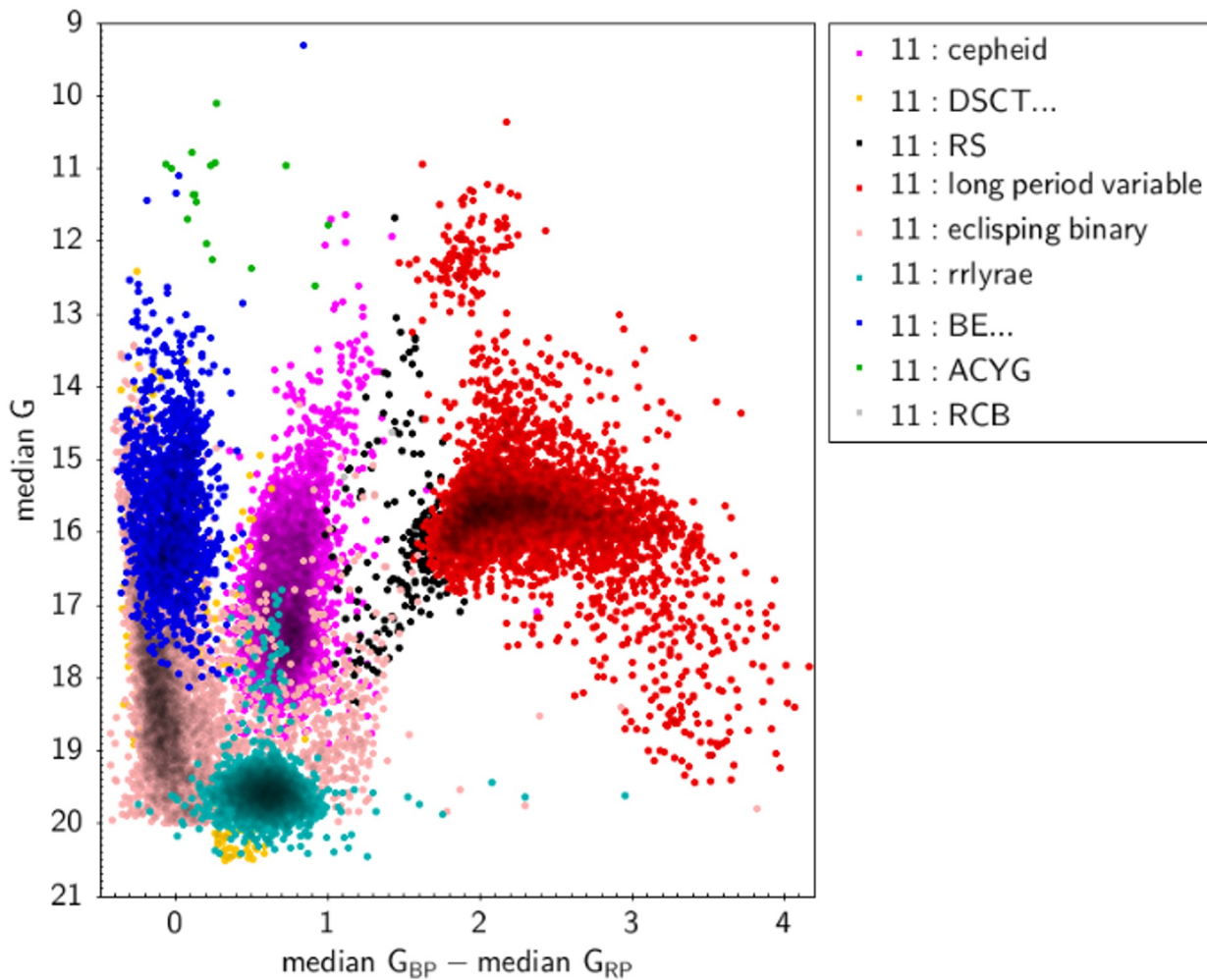
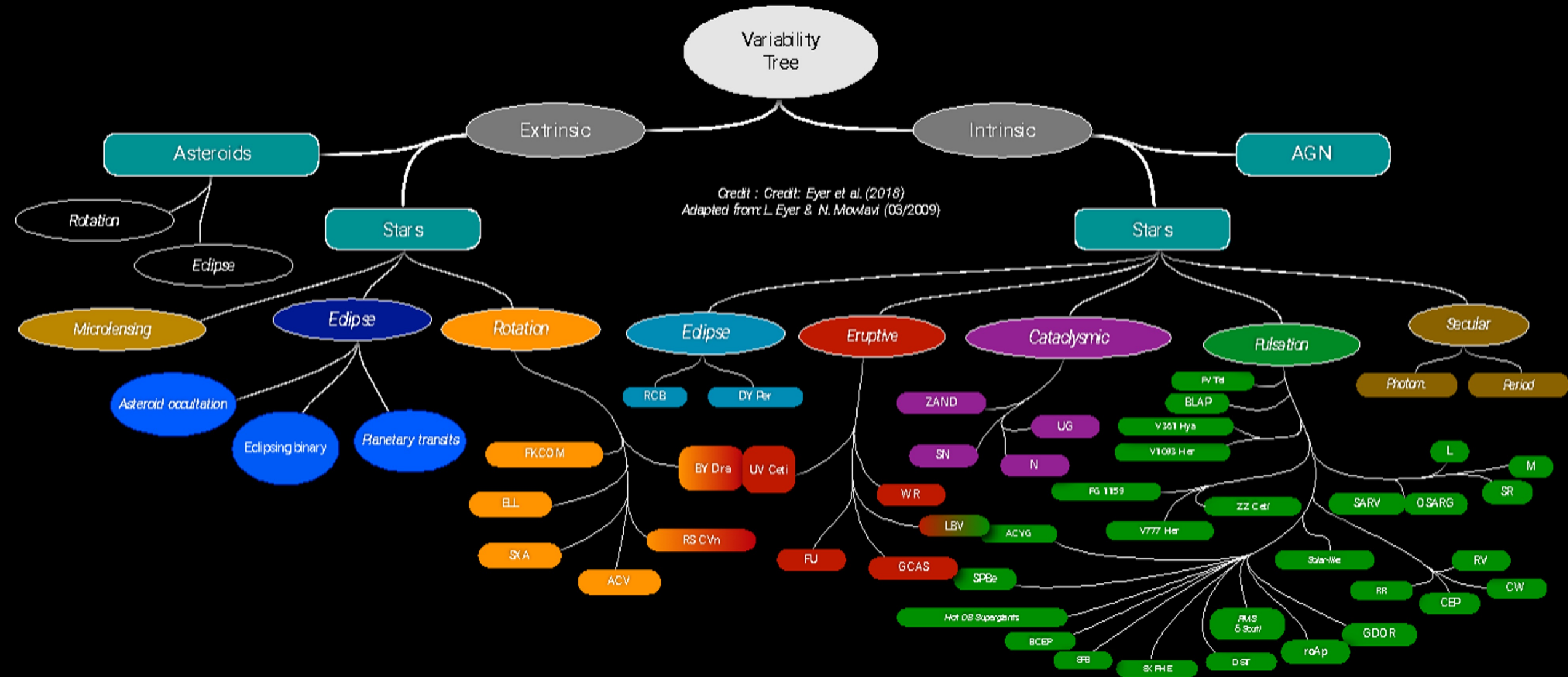


Fig. 4. Pie chart of the main causes of variability from the classification output. The groups are formed by the following types: AGN, Rotation (ACV/.../SXARI, ELL, RS, SOLAR_LIKE), Eruptive/Cataclysmic (BE/.../WR, CV, RCB, SN), Pulsation (ACYG, BCEP, CEP, DSCT/GDOR/SXPHE, LPV, RR, SDB, SPB, WD), Eclipsing systems (ECL, EP), Other (MICROLENSING, S, SYST, YSO).

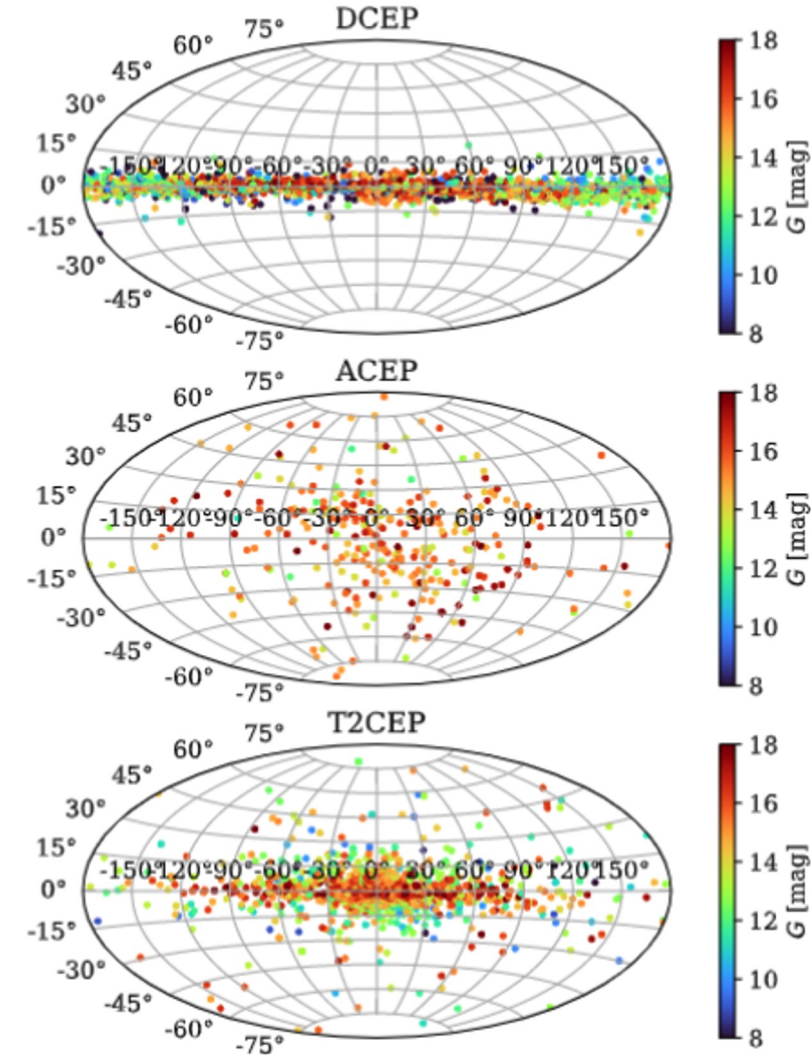
CMD SMC



Variable (pulsating) stars in Gaia DR3



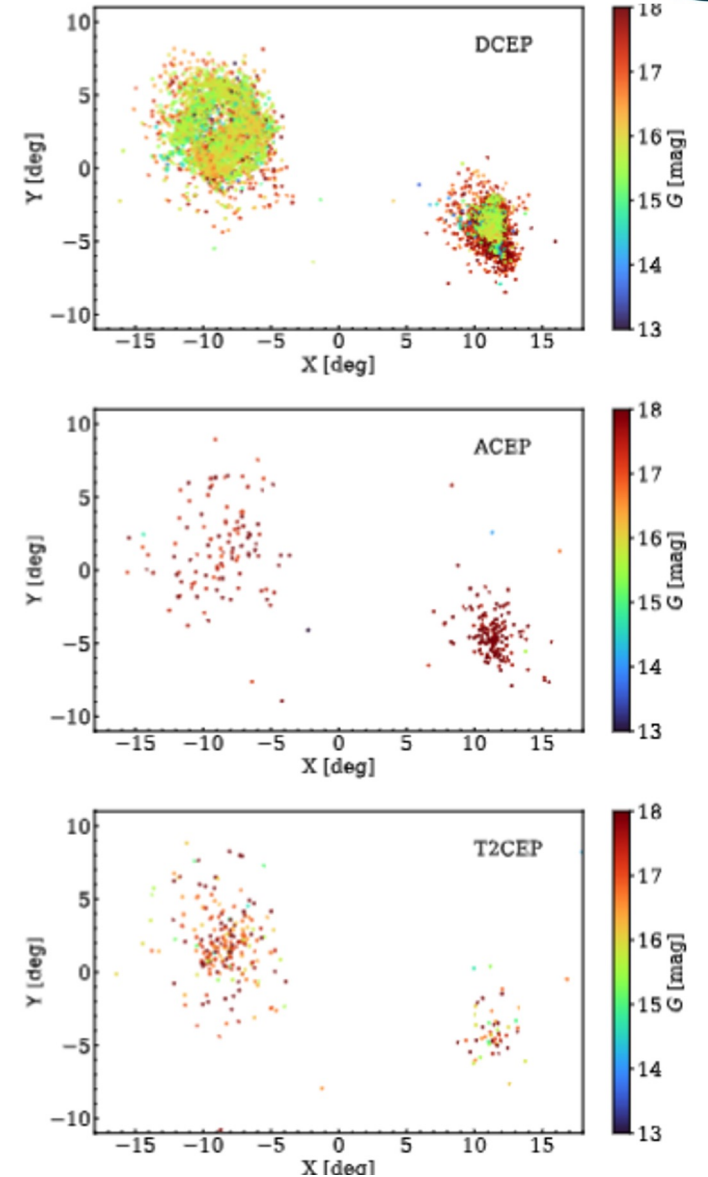
Cepheids in the MW and Magellanic Clouds



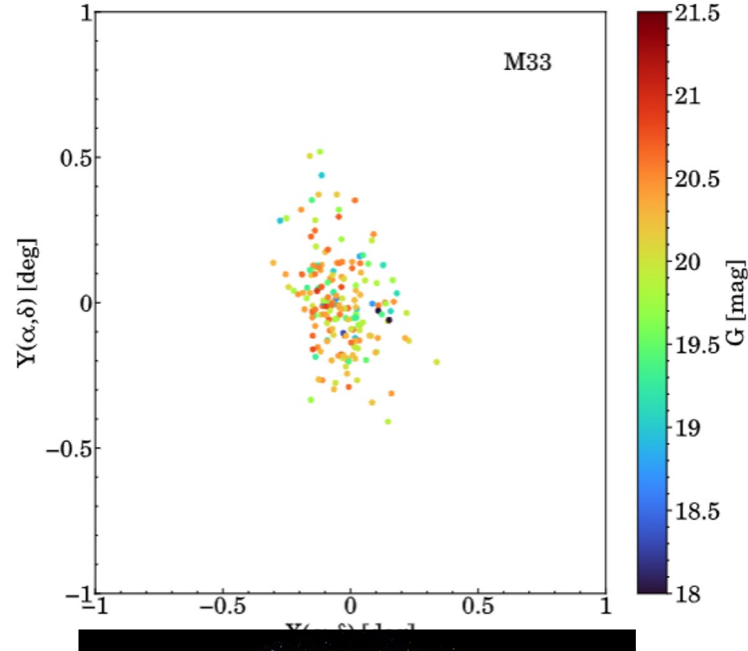
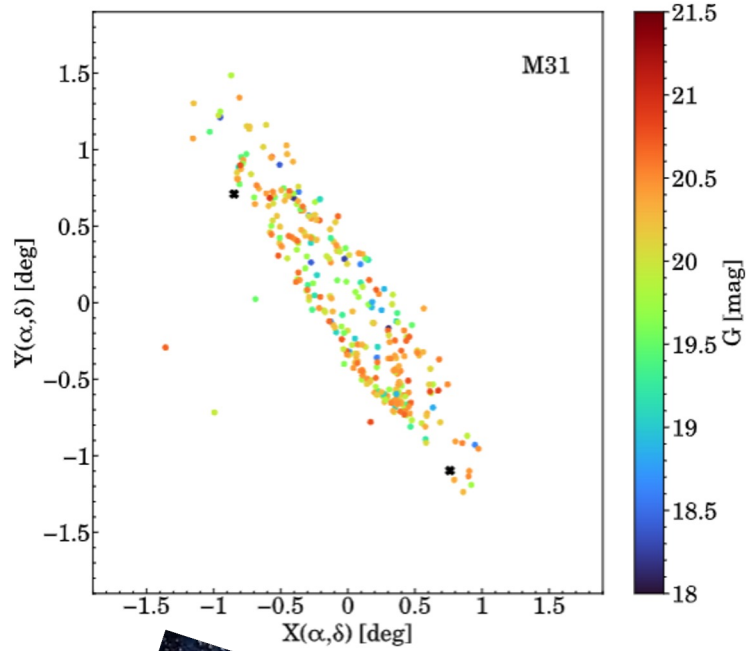
3,434 MW **Classical Cepheids** in Gaia DR3
 → largest homogeneous dataset published so far.

~9,000 Cepheids in the Magellanic Clouds

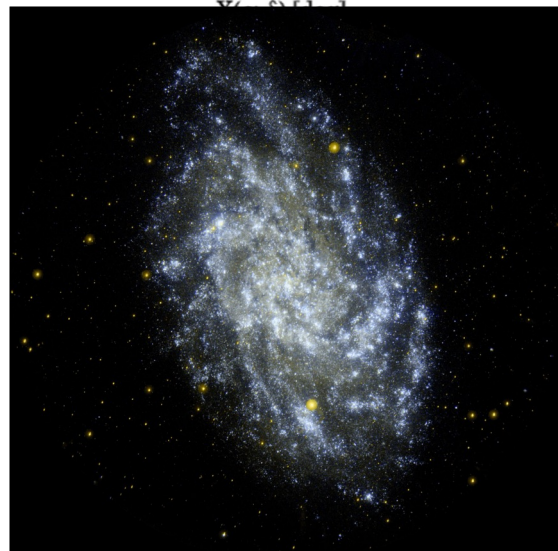
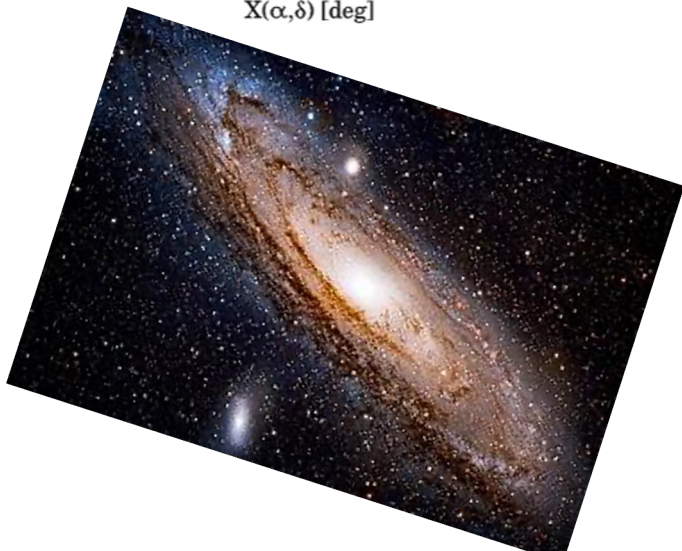
Ripepi et al. 2023, A&A



At the extreme possibility of Gaia: Cepheids in M31 and M33



- 319 Cepheids in Andromeda (M31 ~ 0.750 Mpc)
- 185 Cepheids in Triangulum (M33 ~ 0.840 Mpc)



Ripepi et al. 2023, A&A

Classical Cepheids light curves

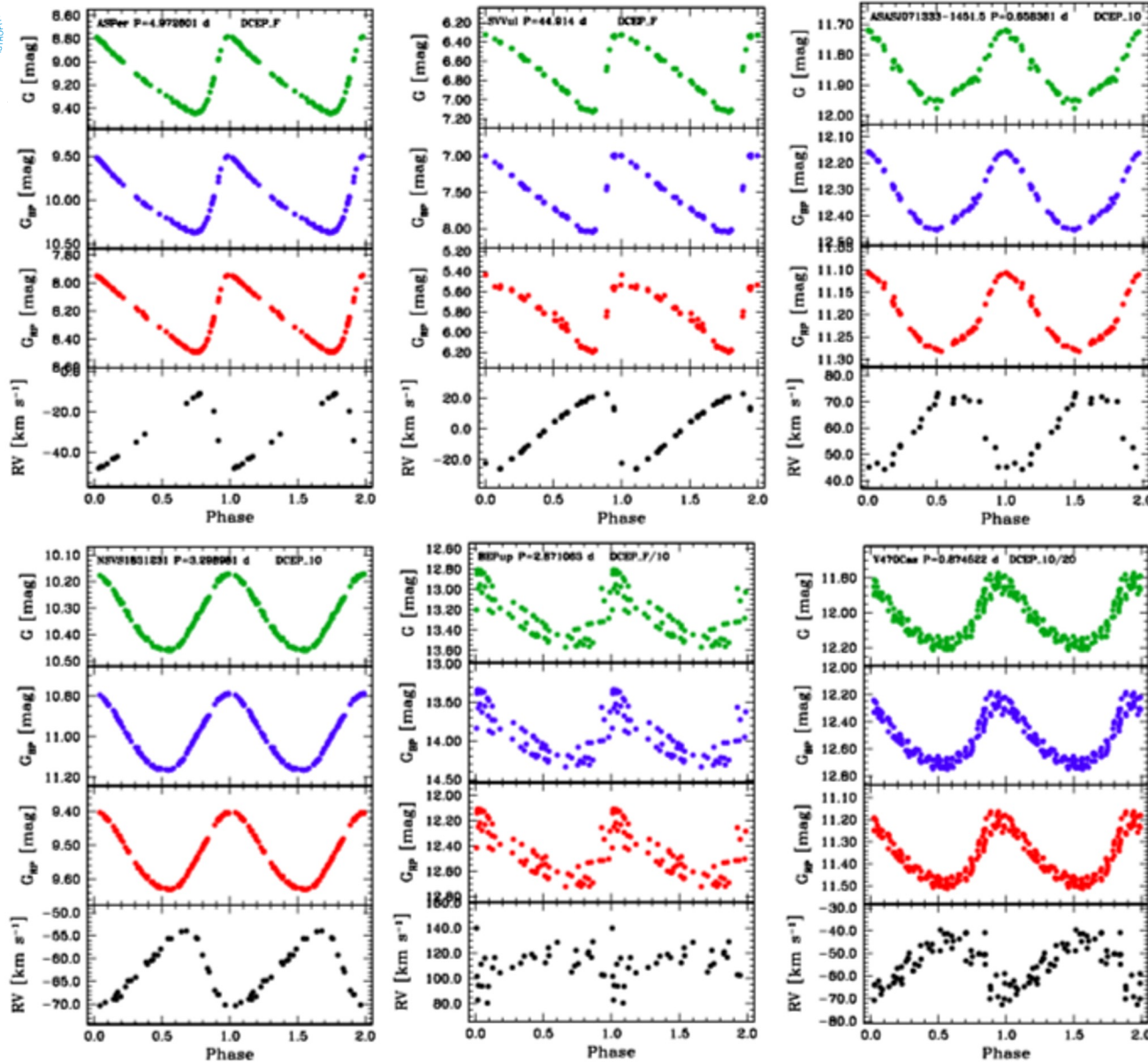
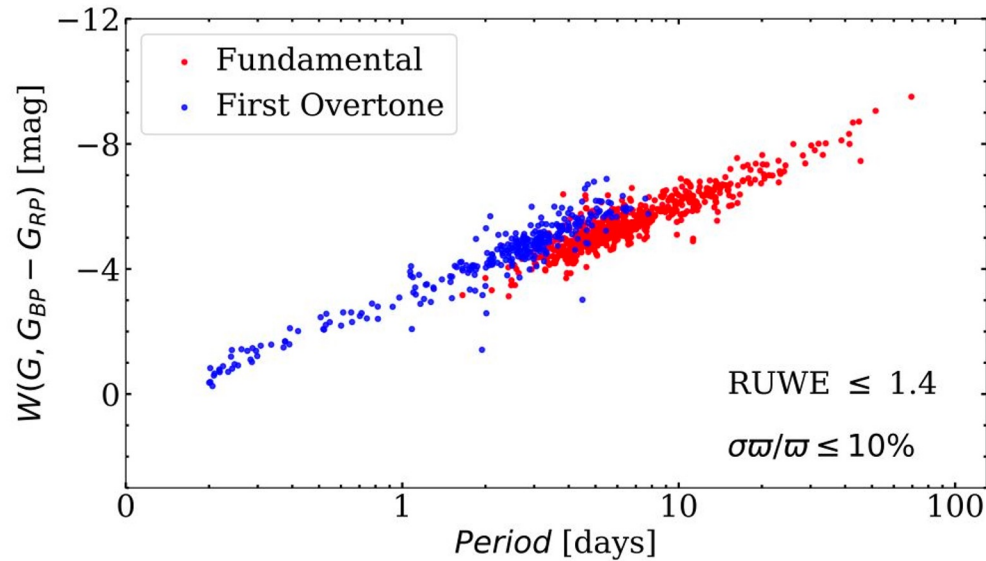


Fig. A.1. Light and RV curves for a selected sample of DCEPs of different modes.

Ripepi et al. 2023, A&A

Period-Luminosity relation of MW Cepheids

Milky Way

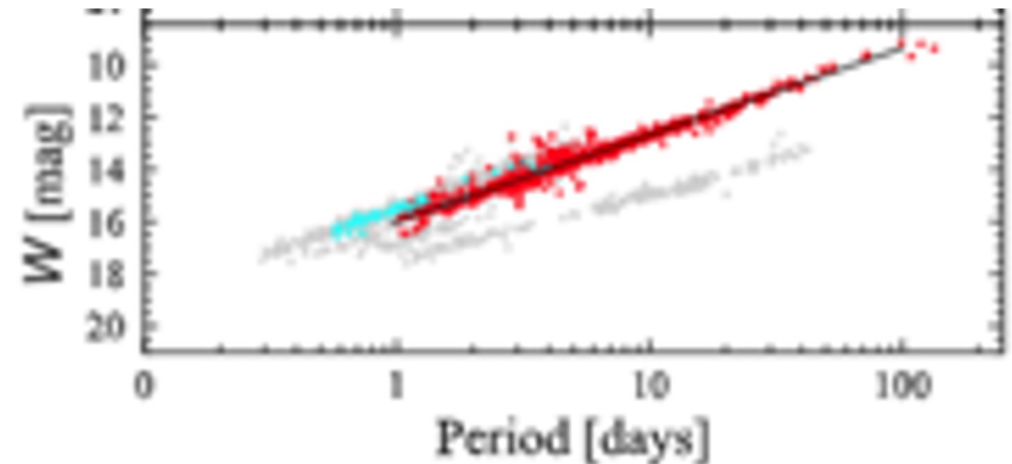


~1060 Cepheids in Gaia DR3 with high-precision parallaxes (distances)

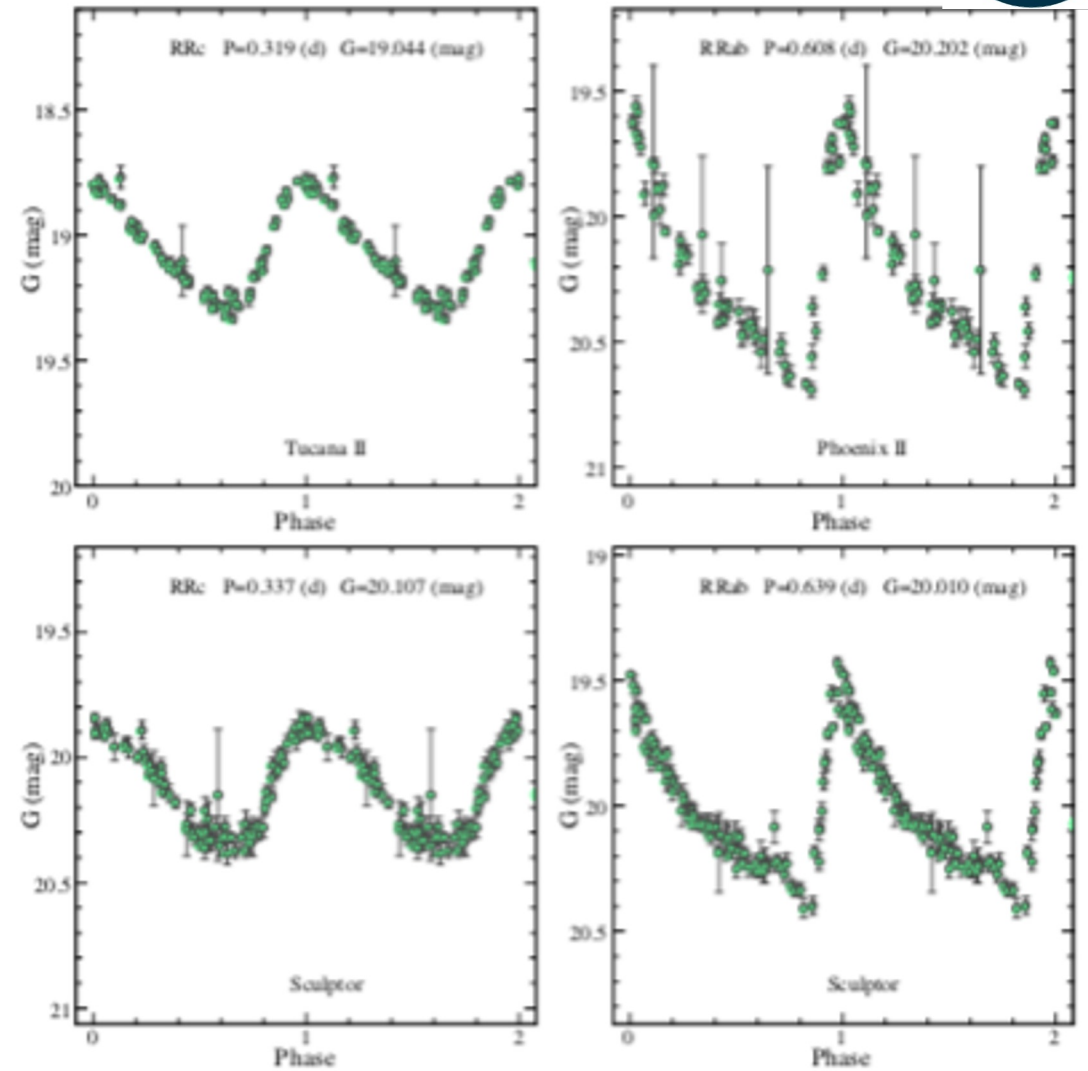
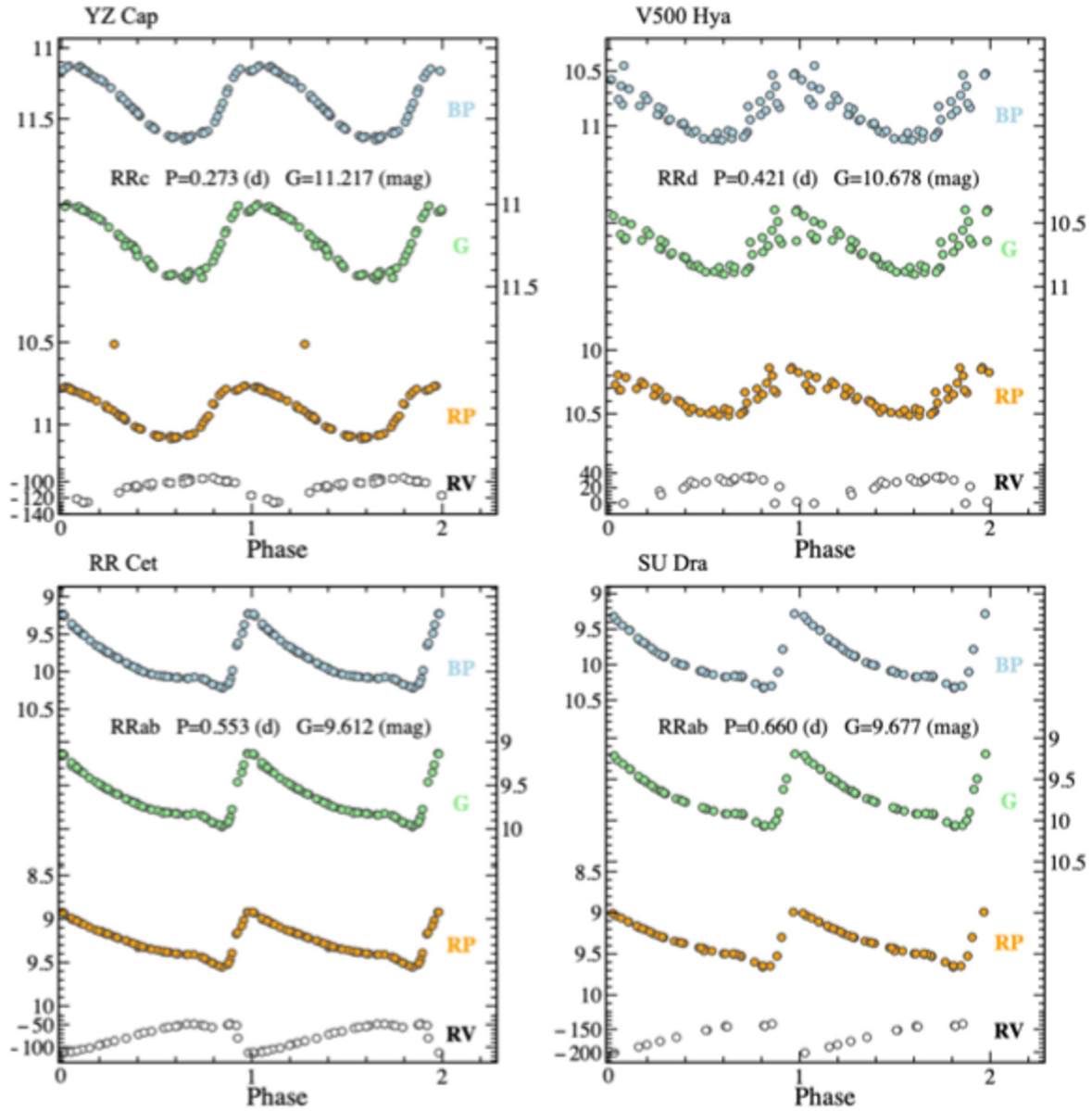
The Period-Luminosity relation constructed with the Gaia measurements (photometry and parallaxes)

→ **calibrate with unprecedented accuracy the first step of the Cosmic distance scale.**

LMC

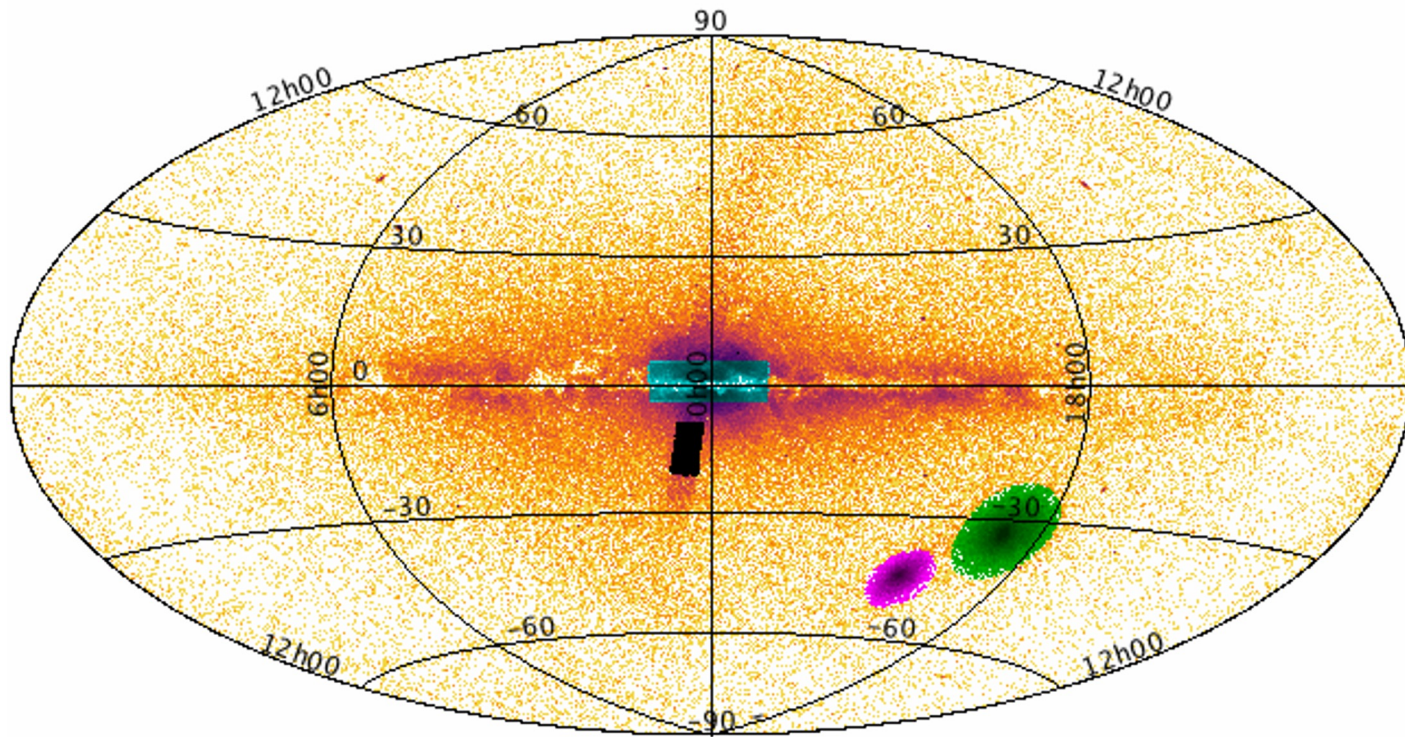


Gaia light curves for RR Lyrae

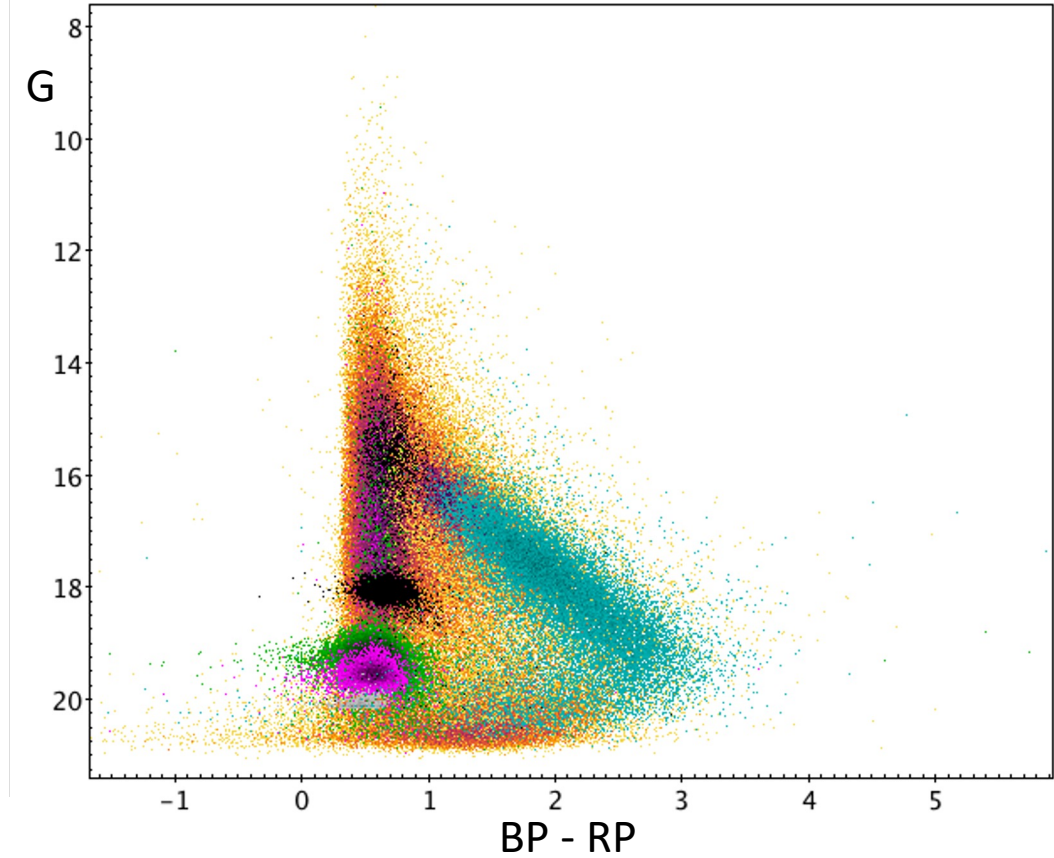


Clementini et al. 2023 A&A

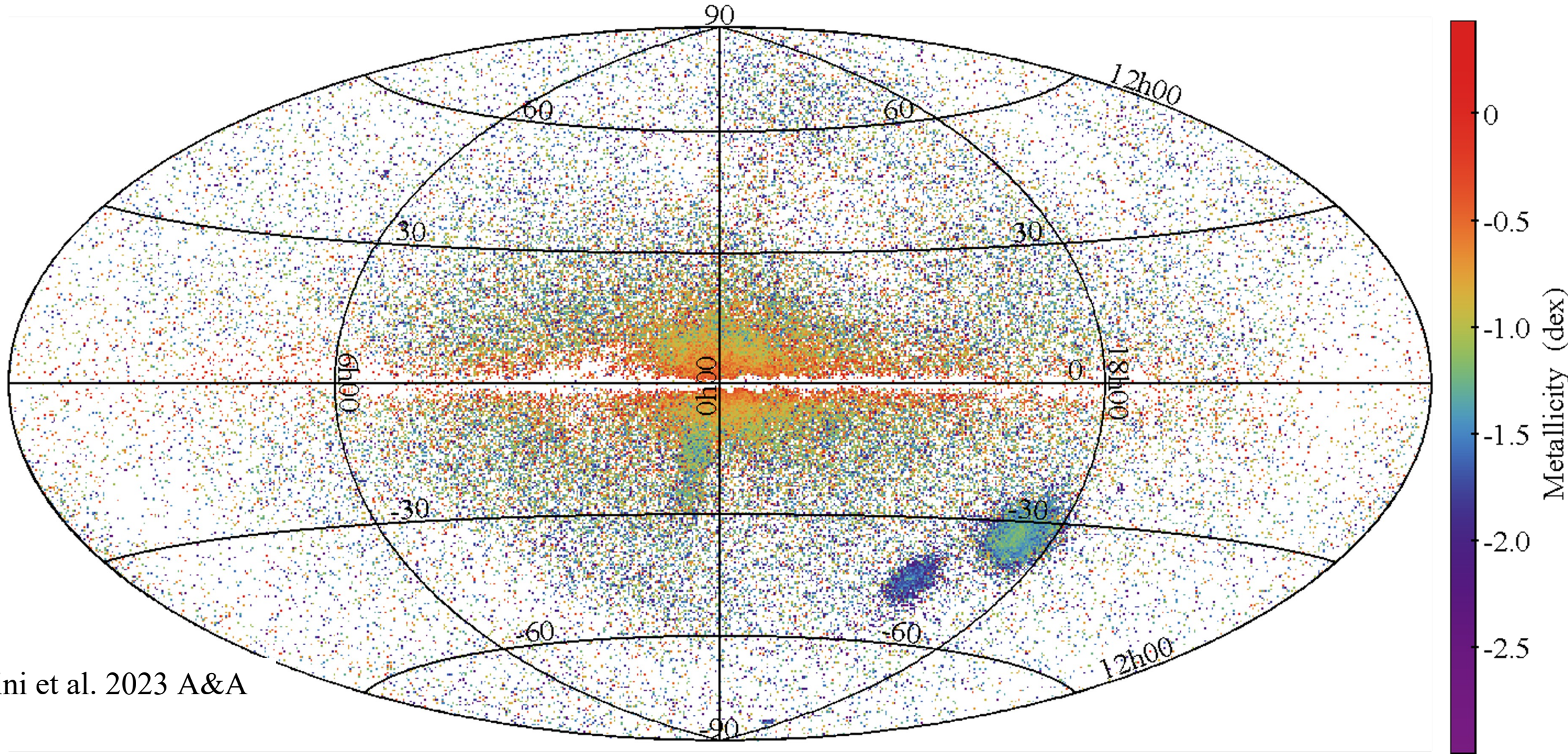
DR3 RR Lyrae Stars: position and CMD



Clementini et al. 2023 A&A

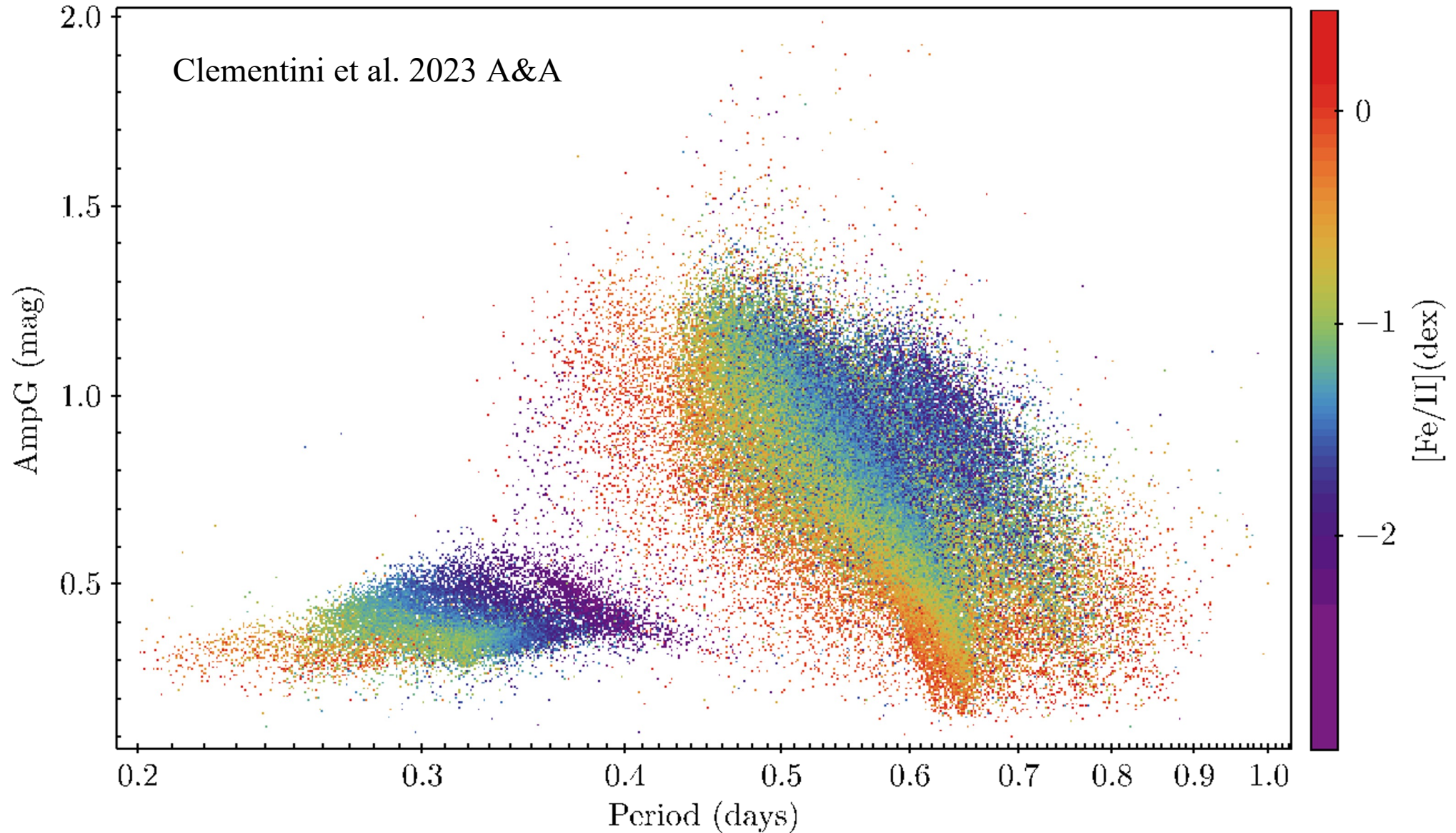


Metallicity for 133.559 RR Lyrae Stars from Fourier parameters



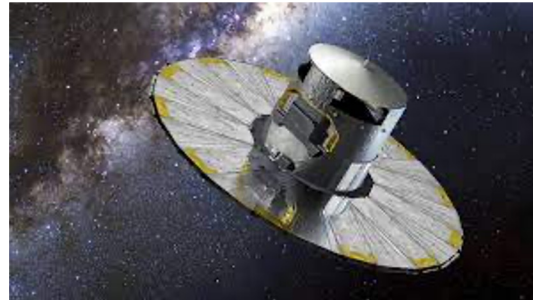
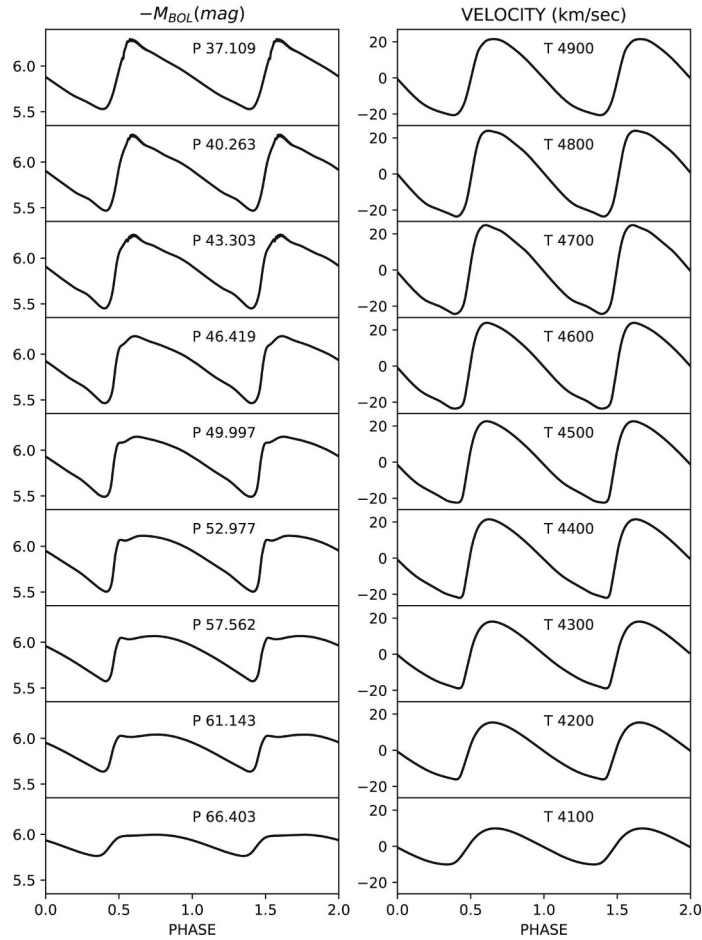
Clementini et al. 2023 A&A

RR Lyrae Period-Amplitude diagram

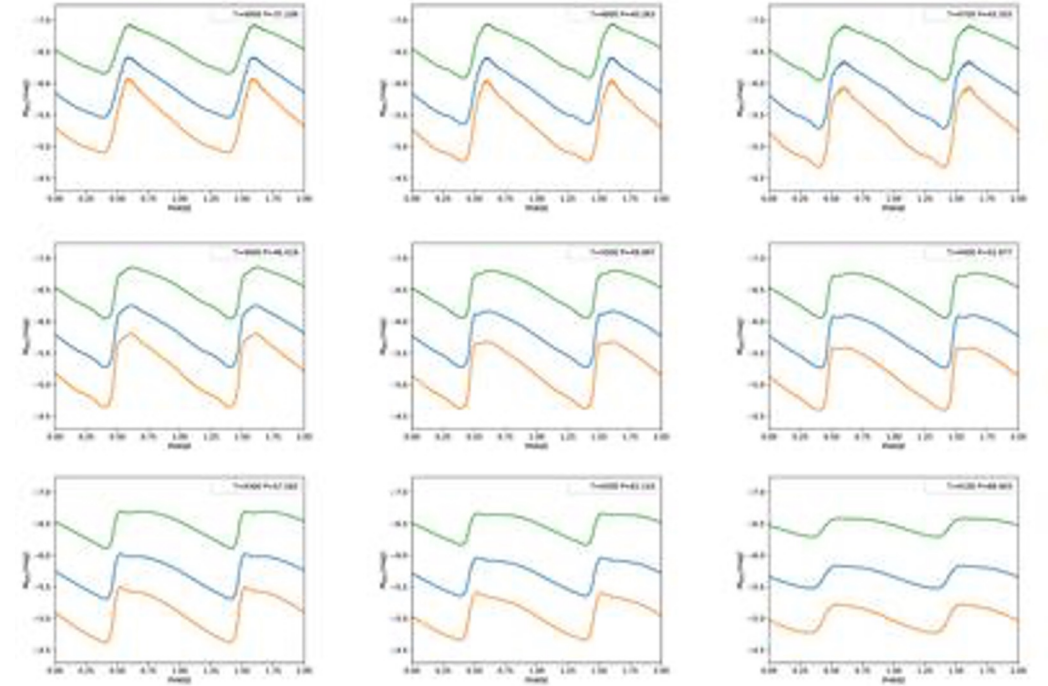


Model predictions for Classical Cepheids in the Gaia filters

$M/M_{\odot} = 11.0$ $\log(L/L_{\odot}) = 4.21$ $\alpha = 1.5$



$M/M_{\odot} = 11.0$ $\log(L/L_{\odot}) = 4.21$ $\alpha = 1.5$



De Somma et al. 2020 ApJS

Cepheid predicted properties in the Gaia filters

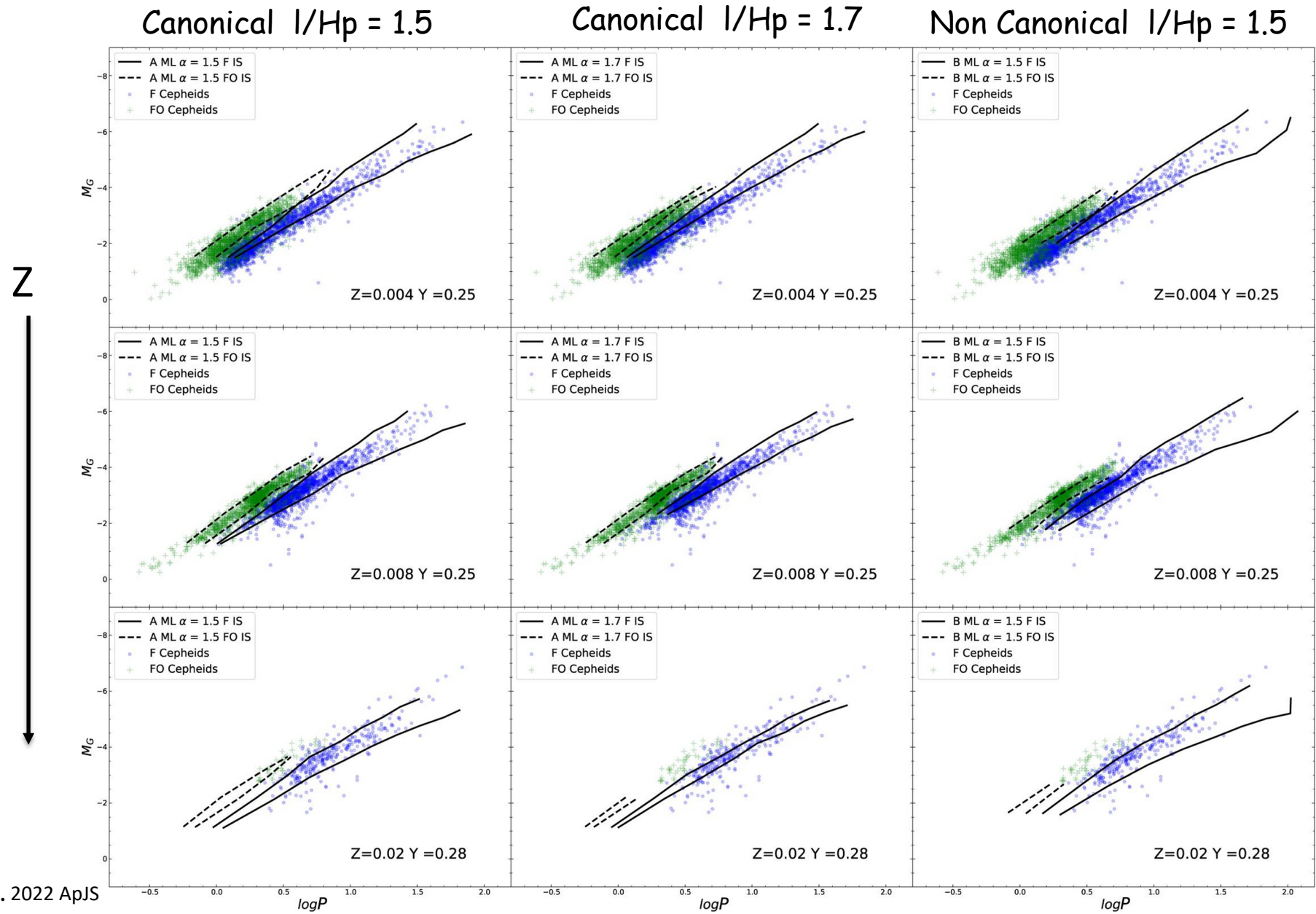
Table 15

Mean Magnitudes and Theoretical Amplitudes in the Gaia DR3 Filters for the Computed F-mode Models with $Z = 0.004$ and $Y = 0.25$, $Z = 0.008$ and $Y = 0.25$, $Z = 0.02$ and $Y = 0.28$, and $Z = 0.03$ and $Y = 0.28$

| Z | Y | M/M_{\odot} | $\log(L/L_{\odot})$ | T_{eff} (K) | α_{ml} | ML | G.m | G.amp | $G_{\text{BP.m}}$ | $G_{\text{BP.amp}}$ | $G_{\text{RP.m}}$ | $G_{\text{RP.amp}}$ |
|-------|------|---------------|---------------------|----------------------|----------------------|----|--------|-------|-------------------|---------------------|-------------------|---------------------|
| 0.004 | 0.25 | 3.0 | 2.49 | 5900 | 1.5 | A | -1.700 | 0.521 | -1.457 | 0.640 | -2.099 | 0.365 |
| 0.004 | 0.25 | 3.0 | 2.49 | 6000 | 1.5 | A | -1.703 | 0.751 | -1.472 | 0.910 | -2.087 | 0.536 |
| 0.004 | 0.25 | 3.0 | 2.49 | 6000 | 1.7 | A | -1.705 | 0.408 | -1.475 | 0.500 | -2.087 | 0.285 |
| 0.004 | 0.25 | 3.0 | 2.49 | 6100 | 1.7 | A | -1.707 | 0.647 | -1.488 | 0.783 | -2.075 | 0.459 |
| 0.008 | 0.25 | 3.0 | 2.39 | 6000 | 1.5 | A | -1.468 | 0.718 | -1.228 | 0.876 | -1.859 | 0.507 |
| 0.008 | 0.25 | 3.0 | 2.59 | 5700 | 1.5 | B | -1.958 | 0.350 | -1.678 | 0.436 | -2.399 | 0.249 |
| 0.008 | 0.25 | 3.0 | 2.59 | 5800 | 1.5 | B | -1.963 | 0.611 | -1.696 | 0.745 | -2.387 | 0.442 |
| 0.008 | 0.25 | 3.0 | 2.59 | 5900 | 1.5 | B | -1.967 | 0.776 | -1.714 | 0.936 | -2.375 | 0.570 |
| 0.02 | 0.28 | 3.0 | 2.32 | 5900 | 1.5 | A | -1.322 | 0.109 | -1.054 | 0.137 | -1.744 | 0.077 |
| 0.02 | 0.28 | 3.0 | 2.32 | 6000 | 1.5 | A | -1.326 | 0.321 | -1.071 | 0.392 | -1.731 | 0.233 |
| 0.02 | 0.28 | 3.0 | 2.32 | 6100 | 1.5 | A | -1.330 | 0.428 | -1.090 | 0.520 | -1.716 | 0.330 |
| 0.02 | 0.28 | 3.0 | 2.32 | 6100 | 1.7 | A | -1.331 | 0.166 | -1.092 | 0.204 | -1.718 | 0.120 |
| 0.03 | 0.28 | 4.0 | 2.68 | 5400 | 1.5 | A | -2.186 | 0.039 | -1.822 | 0.050 | -2.712 | 0.029 |
| 0.03 | 0.28 | 4.0 | 2.68 | 5500 | 1.5 | A | -2.196 | 0.086 | -1.849 | 0.109 | -2.704 | 0.064 |
| 0.03 | 0.28 | 4.0 | 2.68 | 5600 | 1.5 | A | -2.198 | 0.357 | -1.870 | 0.445 | -2.686 | 0.260 |
| 0.03 | 0.28 | 4.0 | 2.68 | 5700 | 1.5 | A | -2.206 | 0.486 | -1.896 | 0.591 | -2.675 | 0.373 |

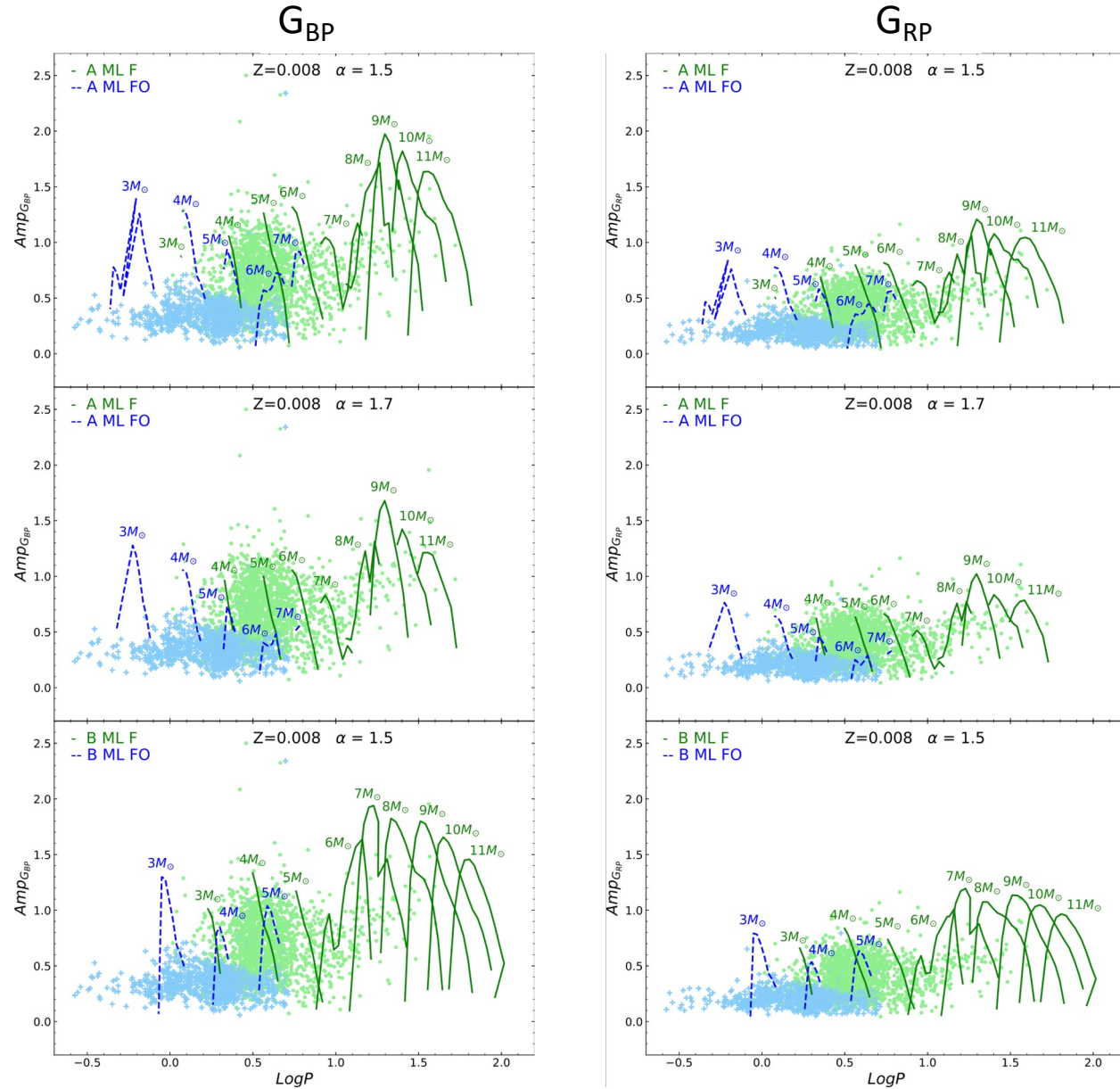
(This table is available in its entirety in machine-readable form.)

Predicted versus observed instability strip in the Period-Gaia magnitude planes



De Somma et al. 2022 ApJS

Predicted versus observed Period-Amplitude planes for LMC Cepheids



De Somma et al. 2022 ApJS

The multi-filter Period-Luminosity-Color and Period-Wesenheit relations in the Gaia filters

For each chemical composition, mean magnitude and colors are adopted together with the periods to infer PLC and PW relations in different filter combinations, including the Gaia bands

$$PLC \rightarrow \langle G \rangle = a + b \log P + c \langle G_{BP} \rangle - \langle G_{RP} \rangle$$

$$PW \rightarrow \langle W \rangle = \langle G \rangle - 1.9 \langle G_{BP} \rangle - \langle G_{RP} \rangle = a + b \log P$$

The metal-dependent Period-Wesenheit relations

$$W = a + b \log P + c [\text{Fe}/\text{H}]$$

Table 19

PWZ Coefficients in the Gaia EDR3 Filters ($W(G, G_{BP}-G_{RP}) = a + b(\log P - 1) + c[\text{Fe}/\text{H}]$) for F and FO CCs Derived by Adopting the A, B, and C ML Relations and $\alpha_{ml} = 1.5, 1.7, \text{ and } 1.9$

| α_{ml} | ML | a | b | c | σ_a | σ_b | σ_c | σ | R^2 |
|---------------|----|--------|--------|--------|------------|------------|------------|----------|-------|
| F | | | | | | | | | |
| 1.5 | A | -6.018 | -3.314 | -0.189 | 0.009 | 0.016 | 0.021 | 0.118 | 0.993 |
| 1.7 | A | -6.072 | -3.379 | -0.129 | 0.010 | 0.016 | 0.021 | 0.090 | 0.996 |
| 1.9 | A | -6.170 | -3.472 | -0.245 | 0.023 | 0.018 | 0.040 | 0.072 | 0.998 |
| 1.5 | B | -5.853 | -3.234 | -0.190 | 0.011 | 0.016 | 0.022 | 0.139 | 0.991 |
| 1.7 | B | -5.871 | -3.262 | -0.260 | 0.012 | 0.015 | 0.023 | 0.118 | 0.995 |
| 1.9 | B | -5.968 | -3.370 | -0.189 | 0.026 | 0.017 | 0.047 | 0.092 | 0.997 |
| 1.5 | C | -5.694 | -3.270 | -0.105 | 0.012 | 0.017 | 0.023 | 0.141 | 0.991 |
| 1.7 | C | -5.722 | -3.274 | -0.140 | 0.012 | 0.015 | 0.022 | 0.116 | 0.994 |
| 1.9 | C | -5.800 | -3.327 | -0.167 | 0.023 | 0.016 | 0.043 | 0.094 | 0.997 |
| FO | | | | | | | | | |
| 1.5 | A | -6.676 | -3.450 | -0.221 | 0.051 | 0.048 | 0.059 | 0.145 | 0.985 |
| 1.7 | A | -6.818 | -3.627 | -0.243 | 0.040 | 0.034 | 0.049 | 0.073 | 0.996 |
| 1.9 | A | -6.933 | -3.688 | -0.349 | 0.045 | 0.030 | 0.052 | 0.034 | 0.999 |
| 1.5 | B | -6.634 | -3.566 | -0.304 | 0.063 | 0.063 | 0.062 | 0.097 | 0.988 |
| 1.7 | B | -6.616 | -3.533 | -0.303 | 0.095 | 0.083 | 0.095 | 0.103 | 0.987 |
| 1.9 | B | -6.719 | -3.627 | -0.304 | 0.066 | 0.050 | 0.068 | 0.030 | 0.998 |
| 1.5 | C | -6.473 | -3.510 | -0.235 | 0.043 | 0.051 | 0.038 | 0.038 | 0.996 |
| 1.7 | C | -6.486 | -3.506 | -0.261 | 0.049 | 0.056 | 0.051 | 0.030 | 0.998 |

De Somma et al. 2022 ApJS

The metal-dependent Period-Wesenheit relations

$$W = a + b \log P + c [\text{Fe}/\text{H}]$$

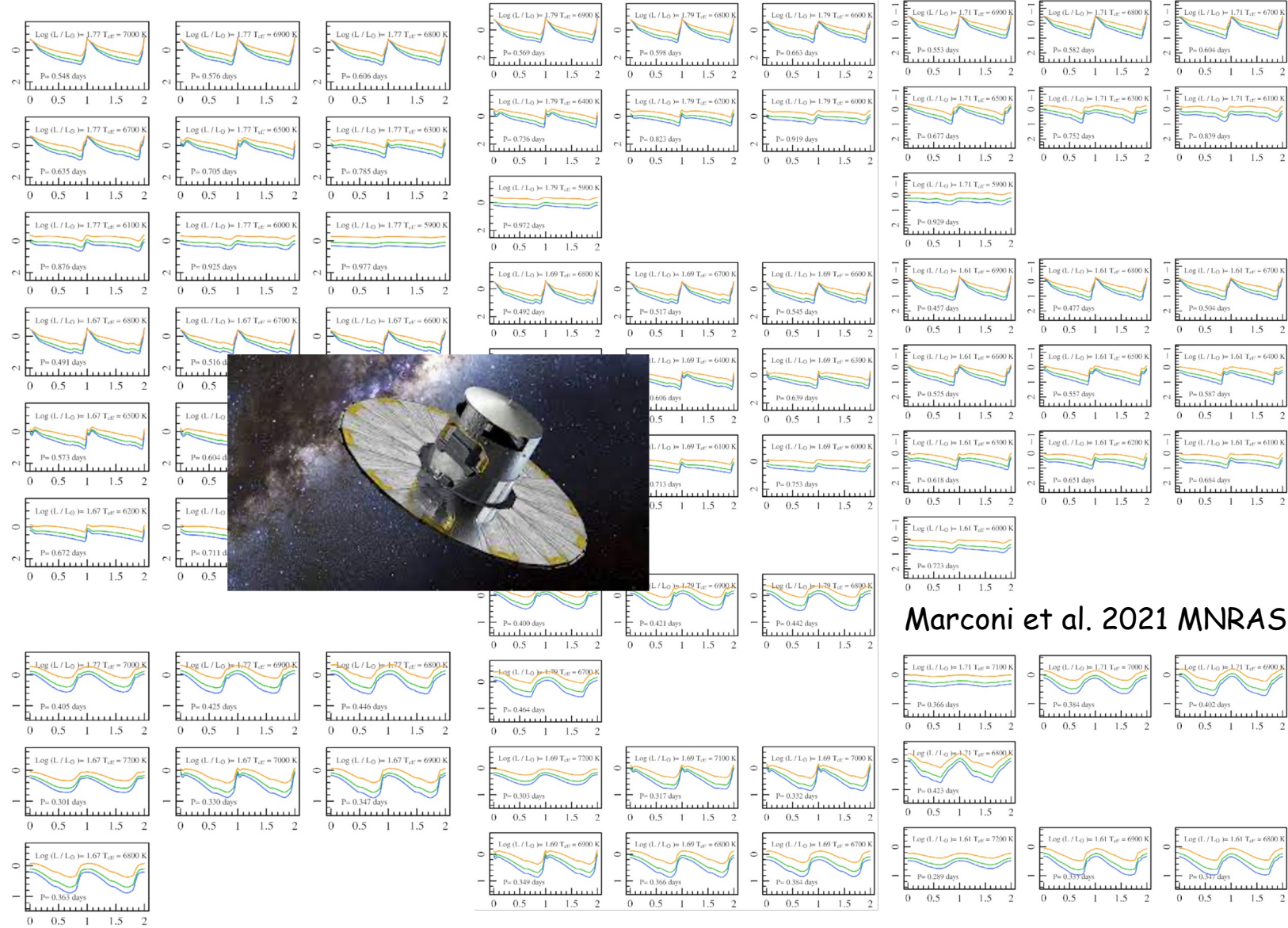
Table 19

PWZ Coefficients in the Gaia EDR3 Filters ($W(G, G_{BP}-G_{RP}) = a + b(\log P - 1) + c[\text{Fe}/\text{H}]$) for F and FO CCs Derived by Adopting the A, B, and C ML Relations and $\alpha_{\text{ml}} = 1.5, 1.7, \text{ and } 1.9$

| α_{ml} | ML | a | b | c | σ_a | σ_b | σ_c | σ | R^2 |
|----------------------|----|--------|--------|--------|------------|------------|------------|----------|-------|
| F | | | | | | | | | |
| 1.5 | A | -6.018 | -3.314 | -0.189 | 0.009 | 0.016 | 0.021 | 0.118 | 0.993 |
| 1.7 | A | -6.072 | -3.379 | -0.129 | 0.009 | 0.016 | 0.021 | 0.118 | 0.993 |
| 1.9 | A | -6.170 | -3.472 | -0.245 | 0.009 | 0.016 | 0.021 | 0.118 | 0.993 |
| 1.5 | B | -5.853 | -3.234 | -0.190 | 0.009 | 0.016 | 0.021 | 0.118 | 0.993 |
| 1.7 | B | -5.871 | -3.262 | -0.260 | 0.009 | 0.016 | 0.021 | 0.118 | 0.993 |
| 1.9 | B | -5.968 | -3.370 | -0.189 | 0.009 | 0.016 | 0.021 | 0.118 | 0.993 |
| 1.5 | C | -5.694 | -3.270 | -0.105 | 0.009 | 0.016 | 0.021 | 0.118 | 0.993 |
| 1.7 | C | -5.722 | -3.274 | -0.140 | 0.009 | 0.016 | 0.021 | 0.118 | 0.993 |
| 1.9 | C | -5.800 | -3.327 | -0.167 | 0.023 | 0.016 | 0.043 | 0.094 | 0.997 |
| FO | | | | | | | | | |
| 1.5 | A | -6.676 | -3.450 | -0.221 | 0.051 | 0.048 | 0.059 | 0.145 | 0.985 |
| 1.7 | A | -6.818 | -3.627 | -0.243 | 0.040 | 0.034 | 0.049 | 0.073 | 0.996 |
| 1.9 | A | -6.933 | -3.688 | -0.349 | 0.045 | 0.030 | 0.052 | 0.034 | 0.999 |
| 1.5 | B | -6.634 | -3.566 | -0.304 | 0.063 | 0.063 | 0.062 | 0.097 | 0.988 |
| 1.7 | B | -6.616 | -3.533 | -0.303 | 0.095 | 0.083 | 0.095 | 0.103 | 0.987 |
| 1.9 | B | -6.719 | -3.627 | -0.304 | 0.066 | 0.050 | 0.068 | 0.030 | 0.998 |
| 1.5 | C | -6.473 | -3.510 | -0.235 | 0.043 | 0.051 | 0.038 | 0.038 | 0.996 |
| 1.7 | C | -6.486 | -3.506 | -0.261 | 0.049 | 0.056 | 0.051 | 0.030 | 0.998 |

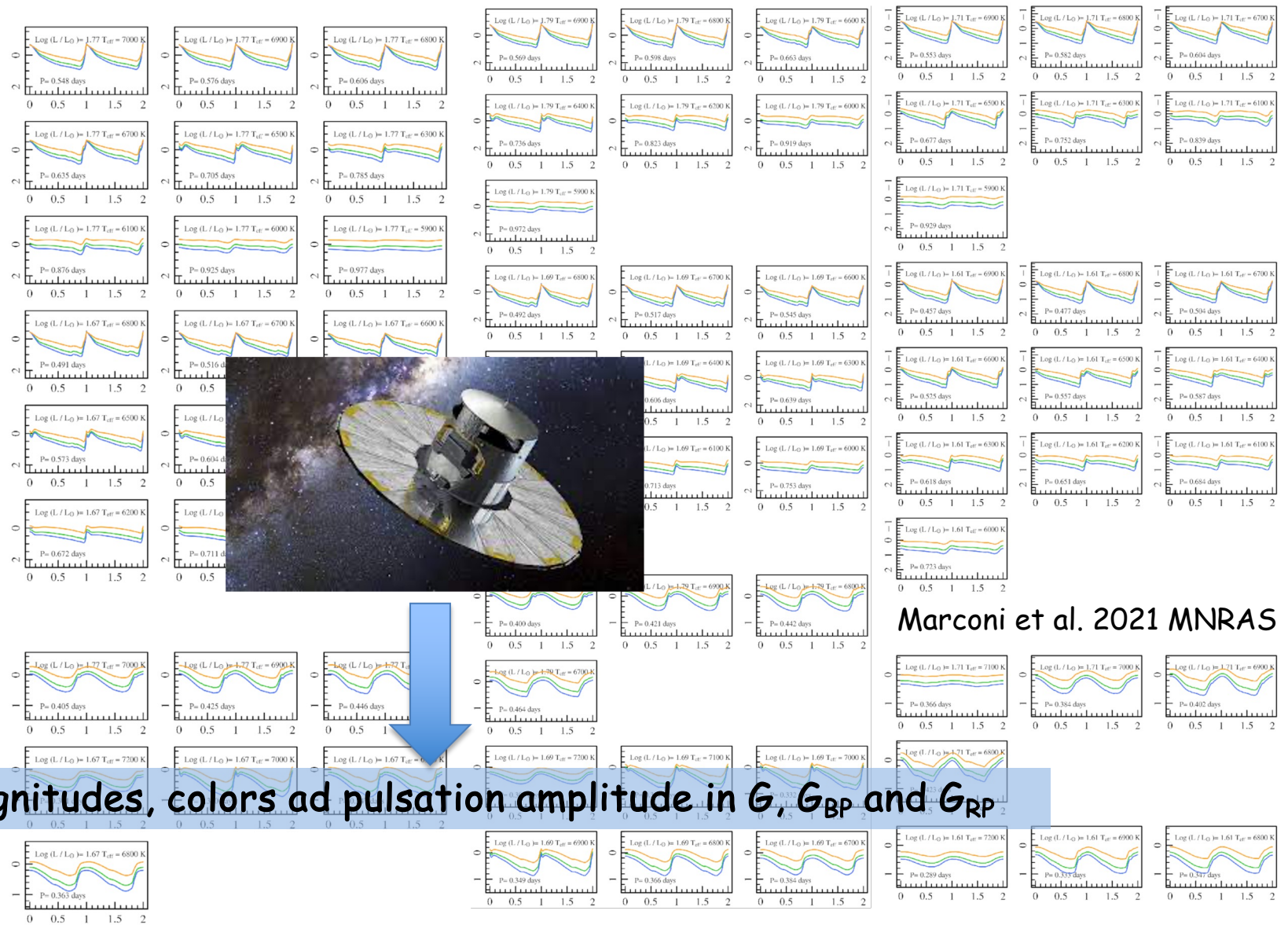
Metal dependent PW relations point towards a metallicity effect on the zero point varying from ~ -0.1 mag/dex to ~ -0.2 mag/dex for the F-mode relations and from ~ -0.1 dex to ~ -0.3 dex for the FO-mode relations.

Model predictions for RR Lyrae in the Gaia filters



Marconi et al. 2021 MNRAS

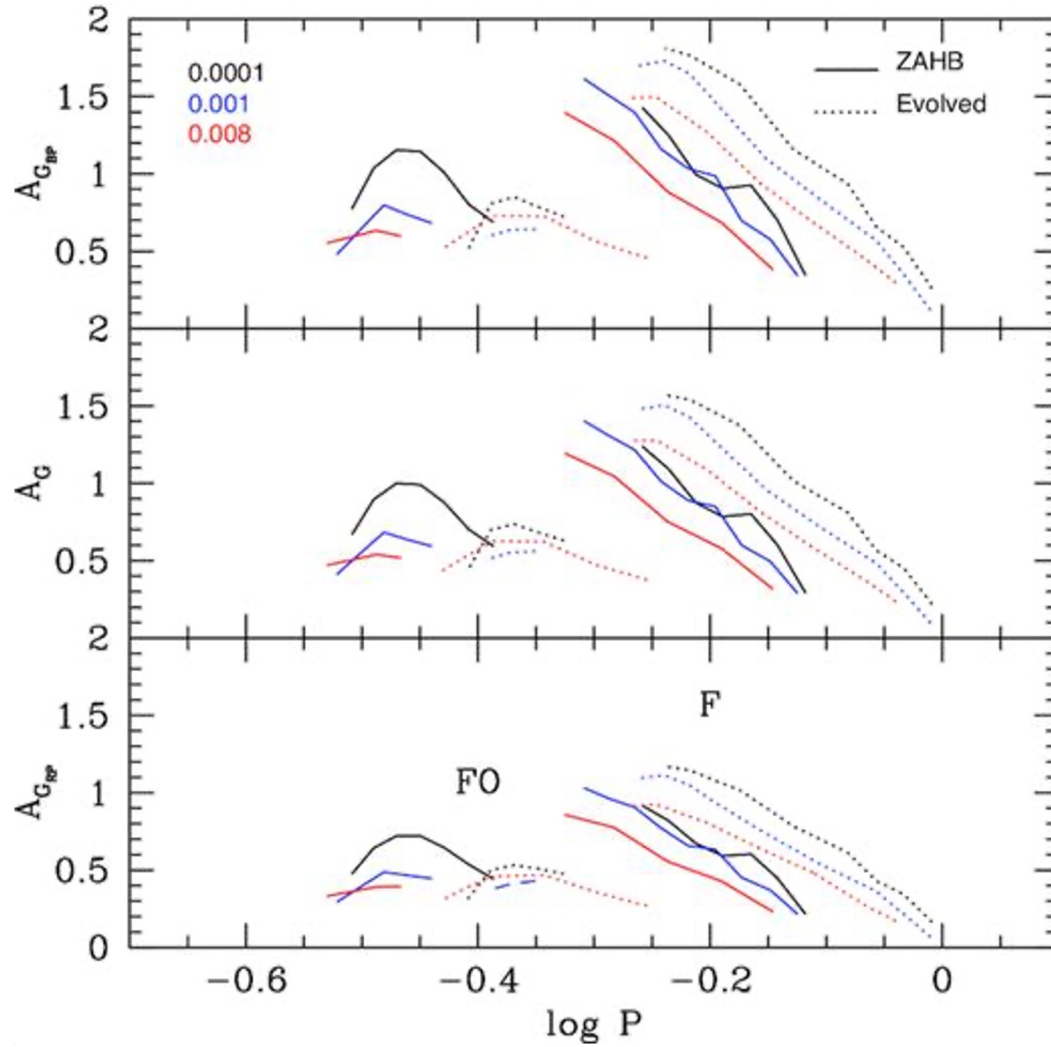
Model predictions for RR Lyrae in the Gaia filters



Marconi et al. 2021 MNRAS

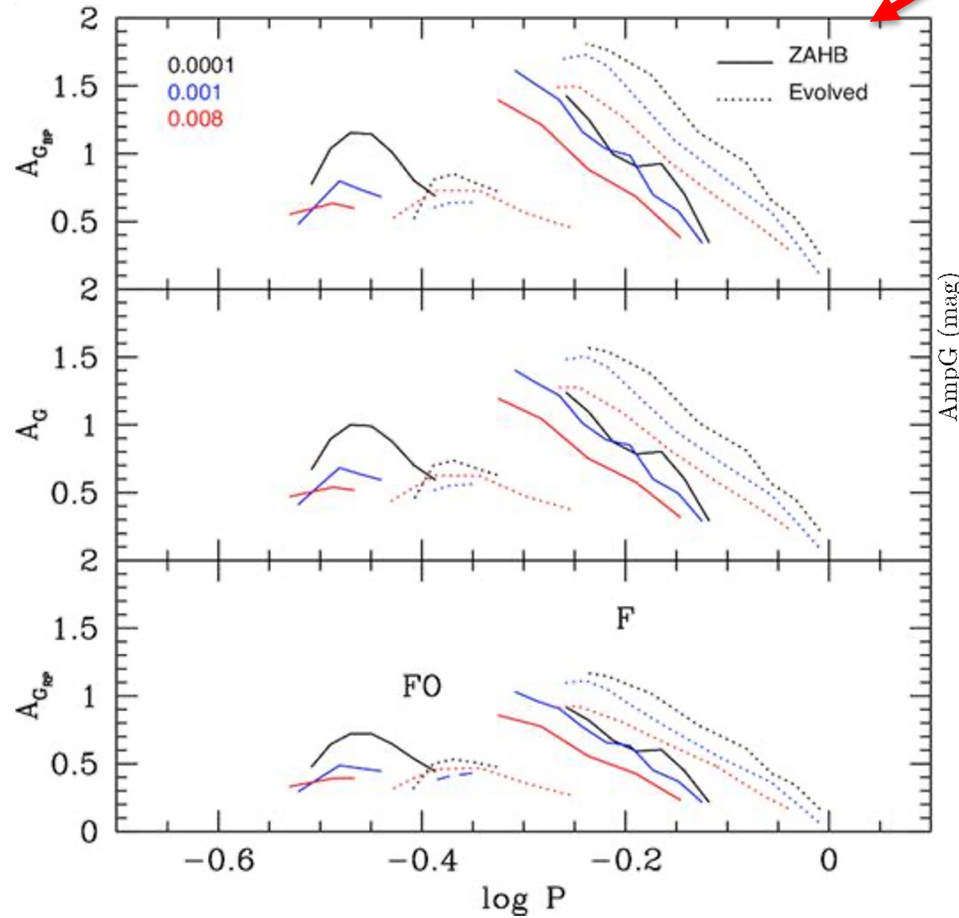
Mean magnitudes, colors and pulsation amplitude in G , G_{BP} and G_{RP}

Model predictions for RR Lyrae in the Gaia filters

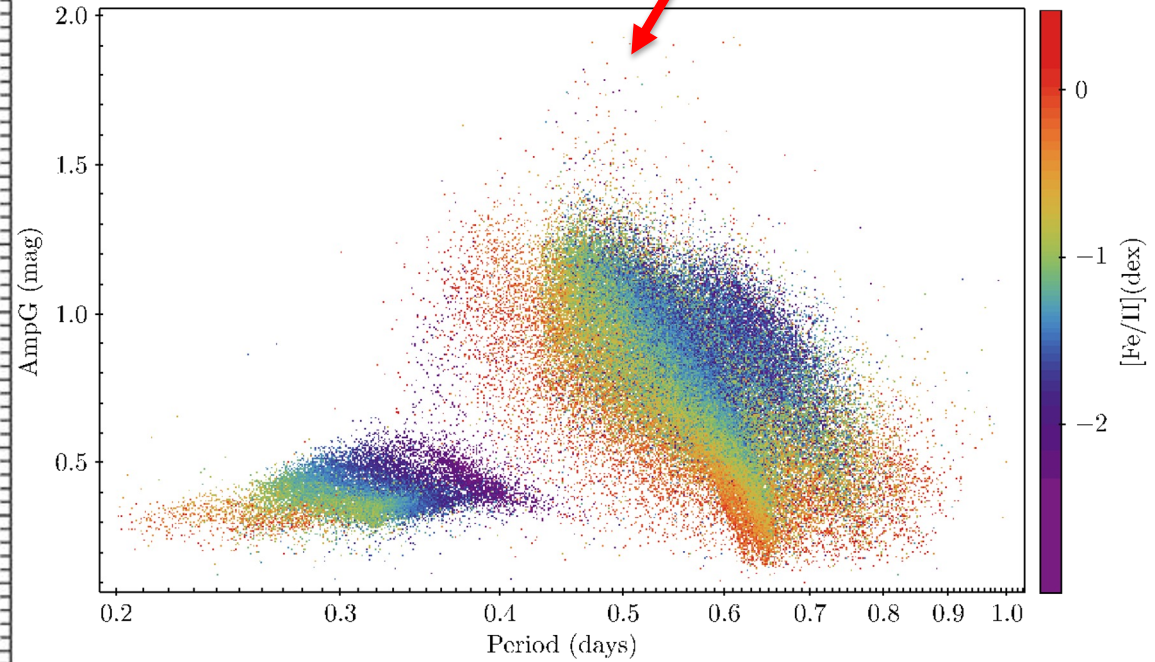


Marconi et al. 2021 MNRAS

The metal abundance effect: Theory versus Observations

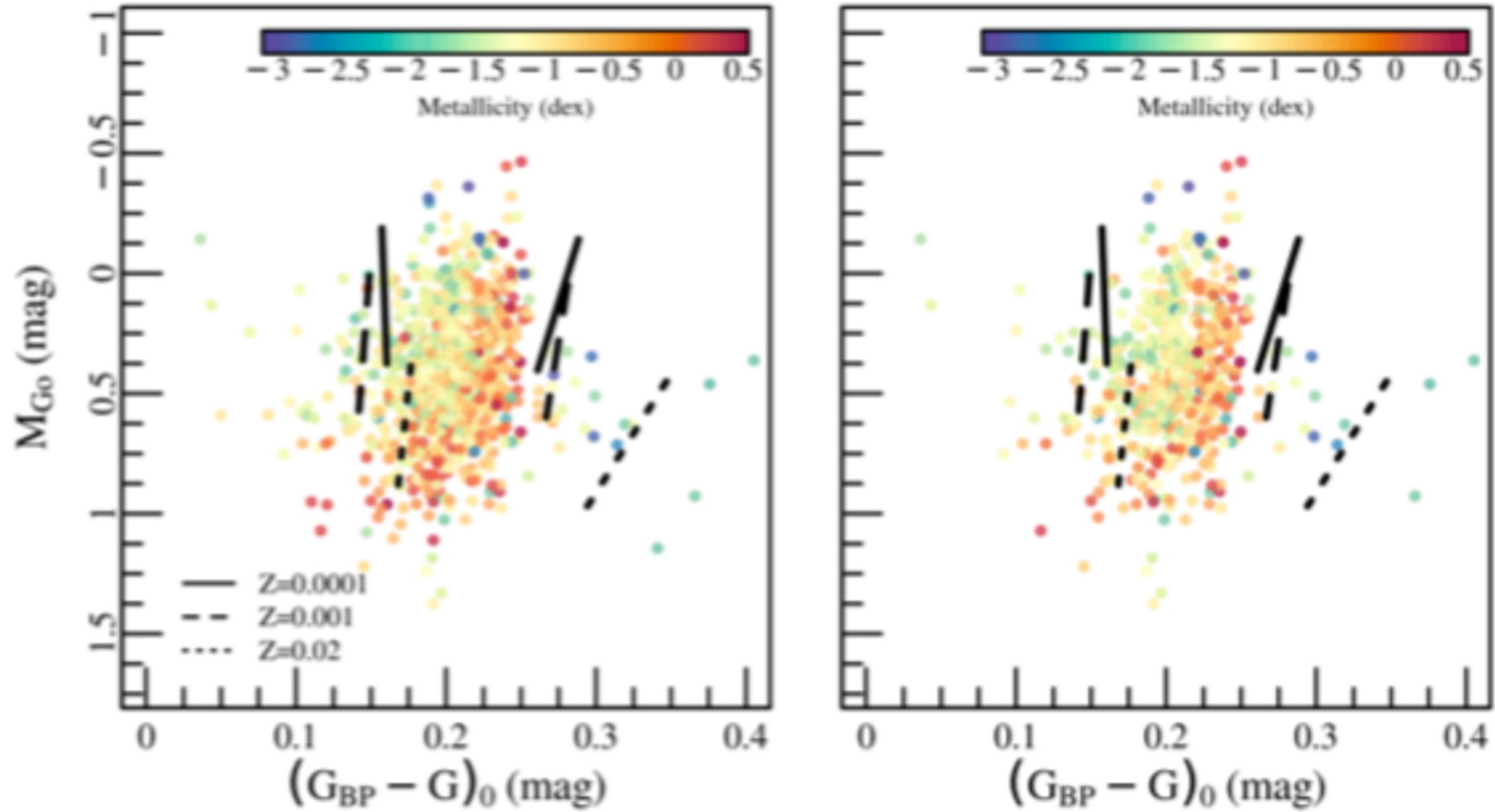


Marconi et al. 2021 MNRAS



Clementini et al. 2023 A&A

Comparison of Gaia data with theoretical RR Lyrae ISs

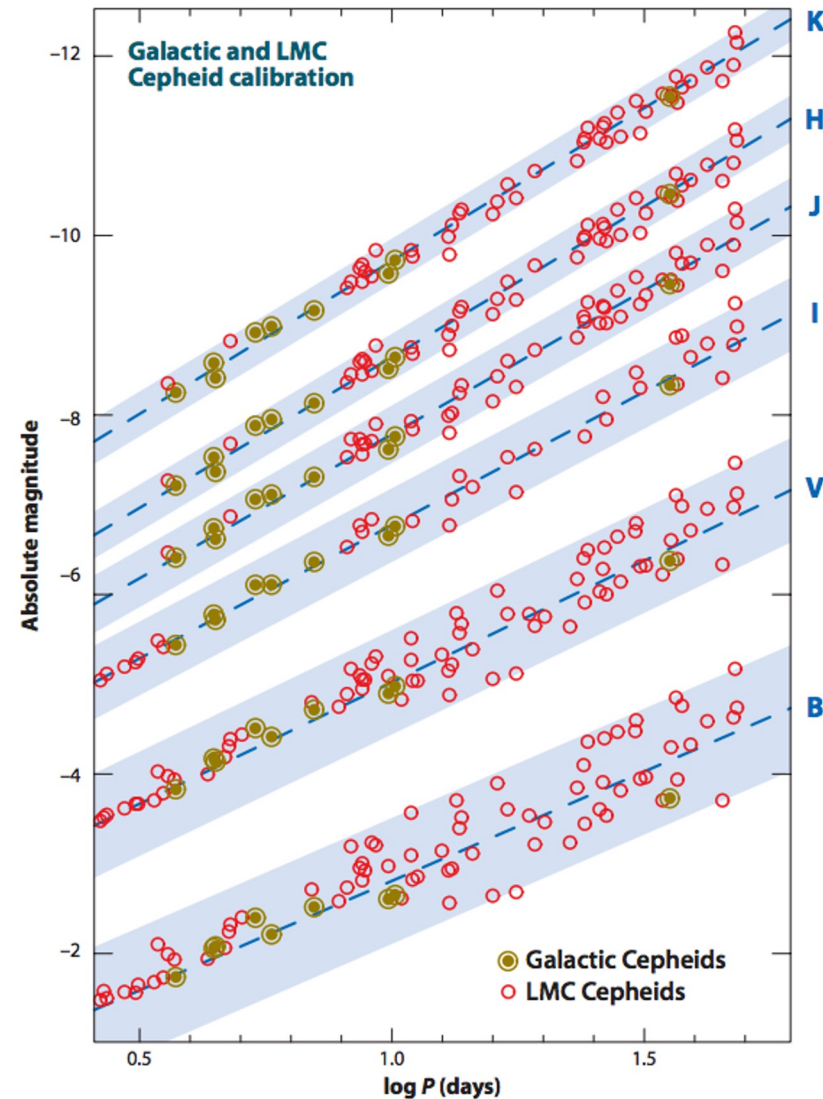


Clementini et al. 2023 A&A

The Gaia-NIR perspective

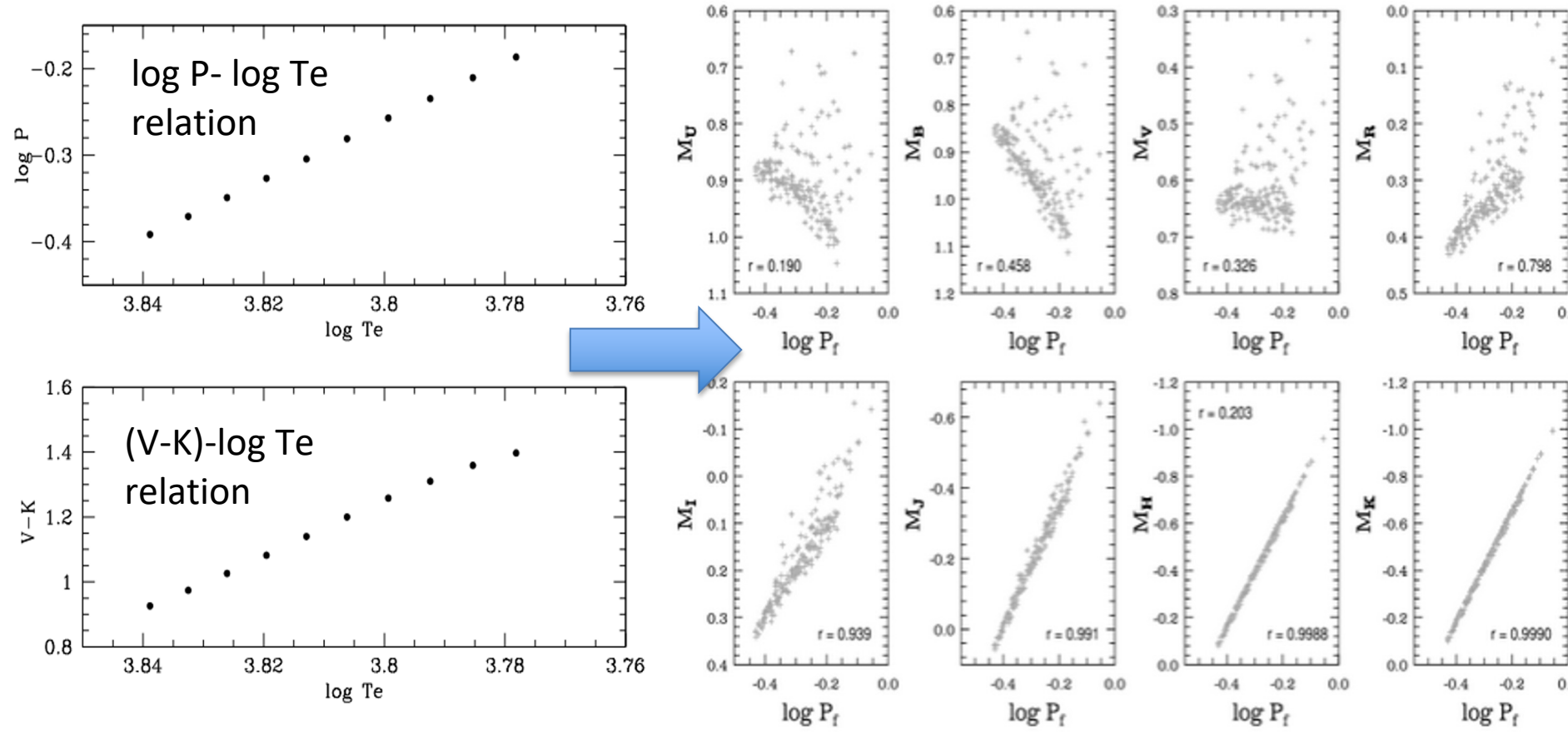
As well known, key uncertainties affecting optical Cepheid PL relations due to the finite width of the instability strip, as well as the ones connected to variable extinction and metallicity, are significantly reduced in the NIR.

Freedman & Madore, 2010



The Gaia-NIR perspective

RR Lyrae obey to strict (metal-dependent) PL relations only in the NIR bands



Bono+2001 MNRAS

Catelan+2004 ApJS

The Gaia-NIR perspective

- Gaia NIR will allow to derive accurate distances of Cepheids and RR Lyrae stars throughout the Galactic plane, including the Galactic bulge, and beyond → thus probing the Galactic components and the spiral arms.
- Gaia NIR will provide additional astrometry separated by 20 years from Gaia → 10-20 times better proper motions and improved parallax determinations also for standard candles such as Cepheids and RR Lyrae.

Conclusions

- Cepheids and RR Lyrae are important standard candles
- Gaia has provided a huge amount of data and information
- Pulsation models based on nonlinear convective computations are able to predict most of the observed properties
- Gaia NIR will allow us to derive precise PL, PLC and PW relations, to improve our calibration of the distance scale and our knowledge of the physics of these pulsating stars.
- The significantly improved proper motions and parallaxes will allow us to probe the Galactic components through and beyond the Bulge.